

## CHAPTER 7

### THE DYNAMIC RESPONSE OF A FREEZE-LINING TO CHANGES IN SLAG BATH COMPOSITION

This chapter, similar to CHAPTER 6, describes a series of experiments conducted with the FLC model. The purpose of these experiments was to study the influence of changes in slag bath composition on the dynamic behaviour of the furnace wall and freeze lining. The same aspects as in CHAPTER 6 were considered:

- Freeze lining thickness.
- Temperature distribution through the furnace wall and freeze lining.
- Time lag in temperature response of the refractory brick wall relative to the time when conditions were changed in the slag bath.
- Liquid slag temperature.
- Composition distribution through the freeze lining.
- Liquid slag composition.

#### 7.1 EXPERIMENTAL SETUP

The flow sheet of the model used for all experiments in this chapter is shown in Figure 89. For the largest part the flow sheet has been documented in paragraph 3.7.1 (page 48). Only the added modules and flow streams are described below.

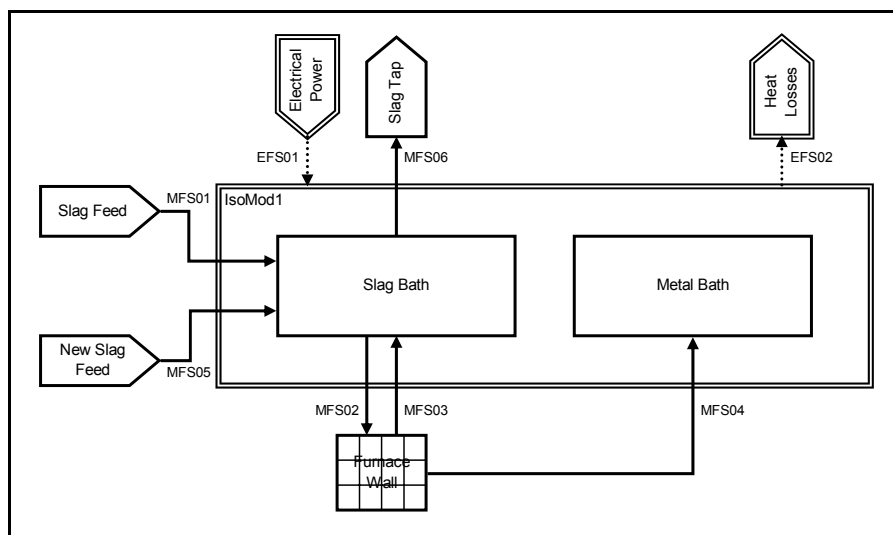


Figure 89 – Flow sheet of the model used for CHAPTER 7 experiments.

- NewSlagFeed

The NewSlagFeed material input module delivers liquid slag that is poured into the SlagBath mixer for the duration of each experiment. The material produced by the NewSlagFeed material input module is discharged into the MFS05 material flow stream.

- MFS05  
The MFS05 material flow stream connects the NewSlagFeed material input module with the SlagBath mixer. It assists in delivering slag to the SlagBath mixer during experiments.
- SlagTap  
The SlagTap material output module extracts liquid slag from the SlagBath mixer for the duration of each experiment. It receives liquid slag via the MFS06 material flow stream.
- MFS06  
The MFS06 material flow stream connects the SlagBath mixer with the SlagTap material output module. It assists in delivering slag to the SlagTap material output module.

The following conditions were common to all experiments:

- An initial liquid slag composition equal of 15%–55%–30% (FeO–TiO<sub>2</sub>–Ti<sub>2</sub>O<sub>3</sub>).
- A liquid slag effective thermal conductivity of 0.005 kW/(m.°C).
- An initial steady state heat flow rate of 250 kW.
- An electrical power input of 250 kW through the ElectricalPower energy input module.
- A heat loss rate of 0 kW through the HeatLosses energy output module.
- An initial freeze lining thickness of 0.102 m.
- An initial freeze lining consisting of only pseudobrookite with a composition of 37.6% FeTi<sub>2</sub>O<sub>5</sub> and 62.4% Ti<sub>3</sub>O<sub>5</sub> (mass basis).

Further, all experiments were run for a period of 24 hours, or until the entire freeze lining had disappeared. During this period slag was introduced into the system at a constant rate through the NewSlagFeed material input module. Slag was removed from the system at the same rate via the SlagTap material output module. This meant that the total mass of slag in the system remained constant throughout the experiments (although the amounts of individual species could vary).

The conditions described above are of course not in complete agreement with conditions in an actual furnace. Slag is produced continuously due to the continuous addition of ilmenite, reductant and energy to the system. Tapping of metal and slag is done in batches. Batch extraction of material could not be modelled with the FLC model presented earlier. The main cause was the decision to represent the freeze lining and wall using only a one-dimensional model. This meant that only phenomena varying along the radial dimension could be studied with the model. Since changes in slag and metal levels in the furnace result in variations in the axial dimension, influences of such variations were automatically eliminated from the set of conditions that the model could be applied to. This was a conscious decision aimed at restricting the scope of work in such a way that it could realistically be completed.

An aspect that must be highlighted is the temperature at which slag was introduced into the system through the NewSlagFeed material input module. This temperature was allowed to vary with the temperature of the slag bath. The new slag therefore entered the system at exactly the same temperature as the slag bath at any point in time. This was done in an attempt to isolate the chemical influence that the new slag would have in the system from possible thermal influences since thermal influences had already been addressed

in CHAPTER 6. By doing this, it is implied that supercooled slag was discharged into the system in some cases.

## 7.2 EXPERIMENTS

The parameters that were varied over the series of experiments include the following:

- Composition of the liquid slag introduced with the NewSlagFeed material input module.
- Residence time of slag in the system. (Given the constant total mass, the residence time is inversely proportional to feed rate.)

The initial steady state heat flow rate fixed the initial temperature distribution in the freeze lining and the initial freeze lining thickness. The set of experiments with the various parameters of interest to each experiment are listed in Table 22 below. The set of experiments consists of 3 subsets.

EXPERIMENT NO.	NEW SLAG COMPOSITION			NEW SLAG FEED RATE	SLAG RESIDENCE TIME
	FeO	TiO <sub>2</sub>	Ti <sub>2</sub> O <sub>3</sub>		
7.1	A	15.0	50.0	35.0	57.5 t/h
7.2	B	15.0	60.0	25.0	57.5 t/h
7.3	C	10.0	55.0	35.0	57.5 t/h
7.4	D	20.0	55.0	25.0	57.5 t/h
7.5	E	10.0	60.0	30.0	57.5 t/h
7.6	F	20.0	50.0	30.0	57.5 t/h
7.7	G	10.0	50.0	40.0	57.5 t/h
7.8	H	20.0	60.0	20.0	57.5 t/h
7.9	I	35.5	59.5	5.0	57.5 t/h
7.10	J	pure stoichiometric ilmenite			4 h
7.11	A	15.0	50.0	35.0	23.0 t/h
7.12	B	15.0	60.0	25.0	23.0 t/h
7.13	C	10.0	55.0	35.0	23.0 t/h
7.14	D	20.0	55.0	25.0	23.0 t/h
7.15	E	10.0	60.0	30.0	23.0 t/h
7.16	F	20.0	50.0	30.0	23.0 t/h
7.17	G	10.0	50.0	40.0	23.0 t/h
7.18	H	20.0	60.0	20.0	23.0 t/h
7.19	I	35.5	59.5	5.0	23.0 t/h
7.20	J	pure stoichiometric ilmenite			10 h
7.21	A	15.0	50.0	35.0	14.38 t/h
7.22	B	15.0	60.0	25.0	14.38 t/h
7.23	C	10.0	55.0	35.0	14.38 t/h
7.24	D	20.0	55.0	25.0	14.38 t/h
7.25	E	10.0	60.0	30.0	14.38 t/h
7.26	F	20.0	50.0	30.0	14.38 t/h
7.27	G	10.0	50.0	40.0	14.38 t/h
7.28	H	20.0	60.0	20.0	14.38 t/h
7.29	I	35.5	59.5	5.0	14.38 t/h
7.30	J	pure stoichiometric ilmenite			16 h

Table 22 – List of experiments conducted for CHAPTER 7.

The same set of 10 new slag compositions was used in each of the three subsets. The distribution of these compositions within the TiO<sub>2</sub>–FeTiO<sub>3</sub>–Ti<sub>2</sub>O<sub>3</sub> ternary system around the initial slag composition is shown in Figure 90. The first eight compositions (A to H) were chosen in such a way that they surrounded the initial slag composition. This would result in the slag bath composition being shifted into these eight surrounding

directions over time. The remaining two compositions were chosen to represent a much less reduced slag (I) and unreduced molten ilmenite (J).

The only parameter that was varied between the three sets is slag residence time. The first set of experiments was done with a residence time of 4 hours. This short residence time and associated extremely high slag feed rate was used to provide an exaggerated view of the influence that changing slag chemistry could have within the system. The second set used a residence time of 10 hours. The associated feed rate is again high, but probably achievable in a unit with the same dimensions as those used in the model. A slag residence time of 16 hours was used in the final set of experiments. This is the most realistic of the three feed rates used.

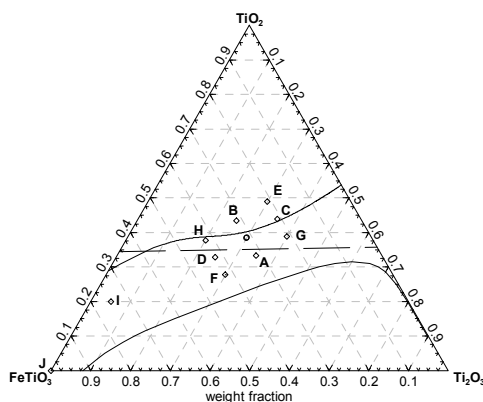


Figure 90 – New slag compositions used in CHAPTER 7 experiments.

The circle indicates the initial slag composition. Diamonds indicate new slag compositions. The dashed line is the  $\text{Ti}_3\text{O}_5$  and  $\text{FeTi}_2\text{O}_5$  (or  $\text{M}_3\text{O}_5$ ) join. The top solid line is the eutectic groove, and the bottom solid line is the slag/slag+  $\text{Fe}^\circ$  phase boundary.

### 7.3 EXPERIMENTAL RESULTS

The results from each experiment are presented below using much the same series of graphs (marked from (a) to (h)) that was used in CHAPTER 6. Only the differences in presentation between CHAPTER 6 and the current chapter are highlighted below. The reader is referred to paragraph 6.3 (page 139) for details about the various graphs. A discussion of the experimental results follows after the graphical presentation of the results of all experiments conducted as part of this chapter.

The top time axis used in graph (e) in CHAPTER 6 was omitted here because the freeze lining showed both an increase and a decrease in thickness in most of the experiments. It was therefore not possible to use such an axis to give an indication of time on these graphs. To be able to use the same axes in all cases, graph (e) was drawn for freeze lining thickness values from zero, even in cases where the freeze lining thickness did not reach zero during the simulation.

In cases such as experiments 7.2 and 7.3 the liquid slag composition crossed the eutectic groove towards the  $\text{TiO}_2$  corner of the ternary diagram. This caused rutile to become the primary solidification phase. When

this happens, graph (e) shows the freeze lining at the solid-liquid interface as consisting of mostly  $\text{TiO}_2$  with a small amount of  $\text{Ti}_2\text{O}_3$  dissolved in the rutile matrix.

Graph (e) is not provided for experiments 7.20 and 7.30 because virtually the entire freeze lining had melted away by the end of these experiments.

Two fixed compositions are highlighted on graph (f). The initial liquid slag composition is shown as a circle, and the composition of the new liquid slag with a diamond. This was done to give the reader perspective about the change in liquid slag composition relative to these two points.

## 7.3.1 Experiment 7.1

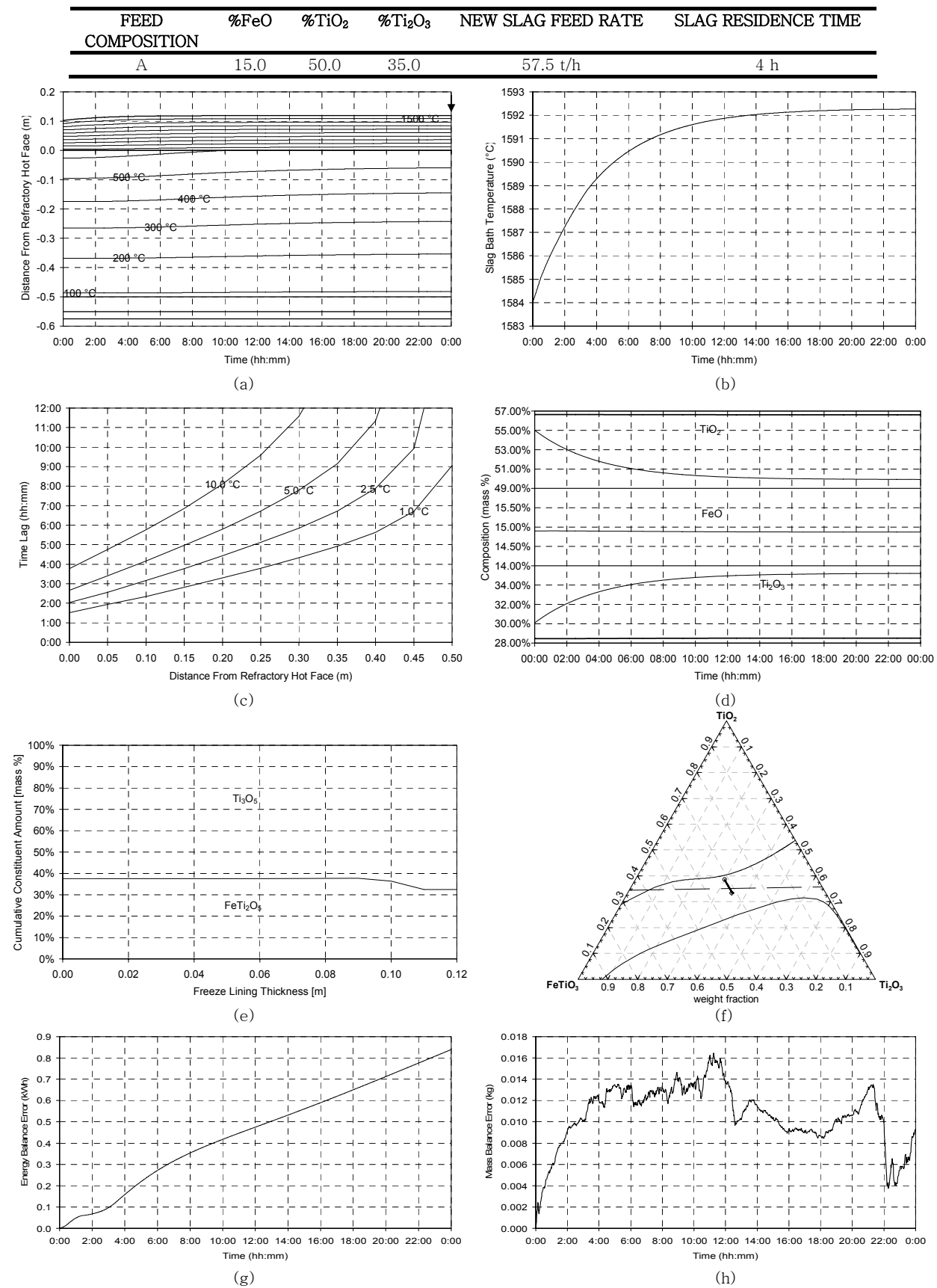


Figure 91 – Experiment 7.1 results.

## 7.3.2 Experiment 7.2

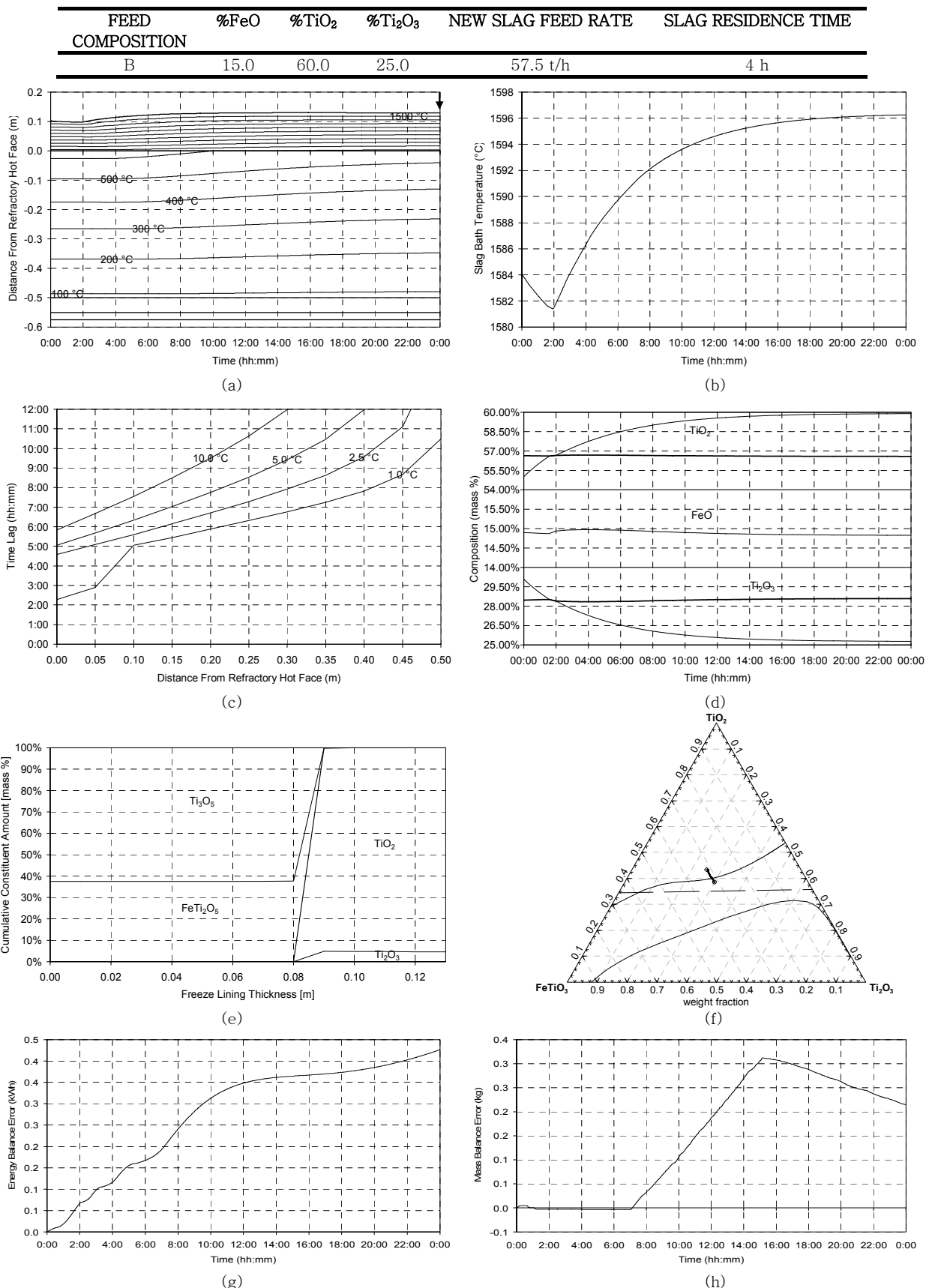


Figure 92 – Experiment 7.2 results.

### 7.3.3 Experiment 7.3

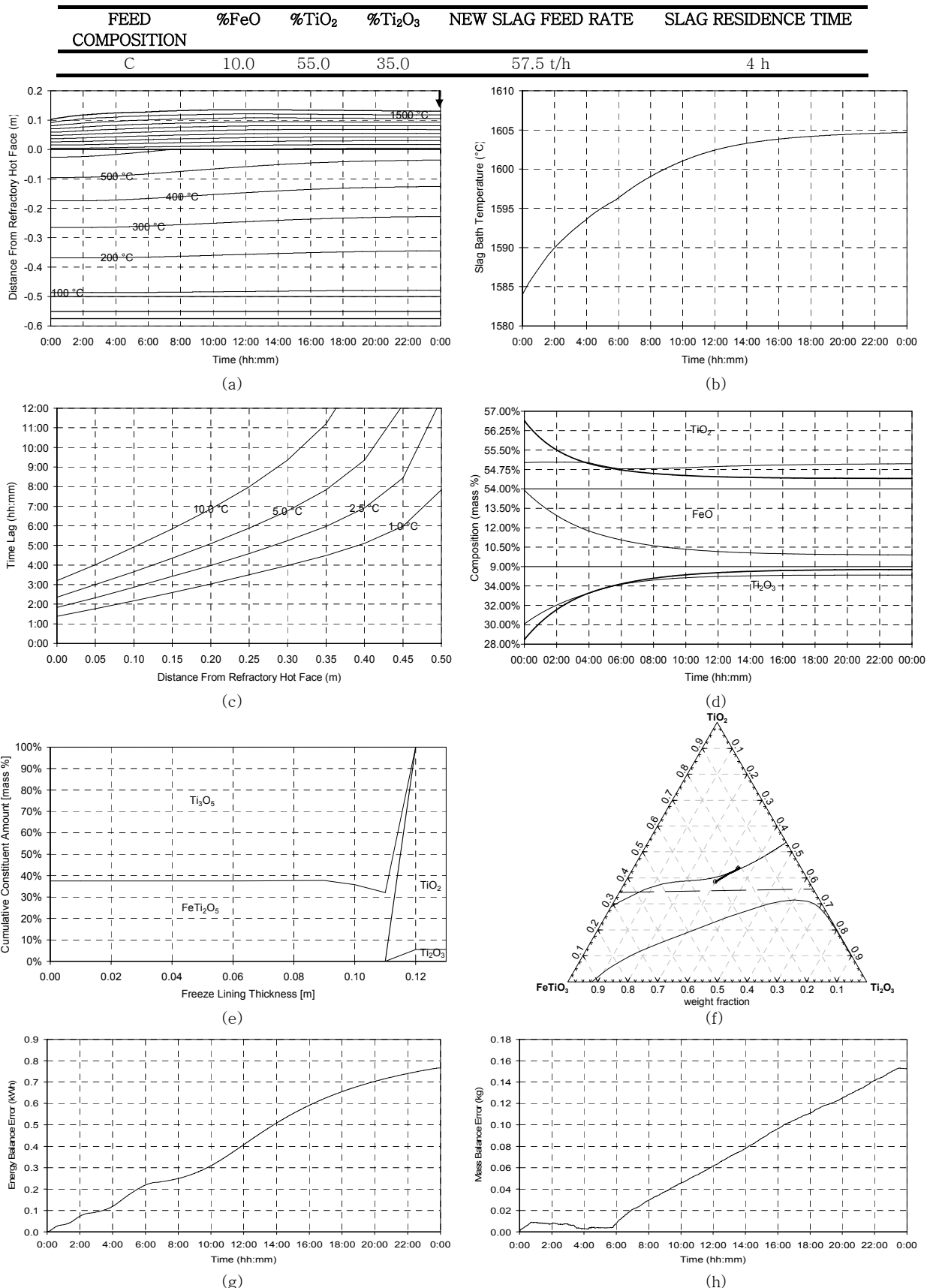


Figure 93 – Experiment 7.3 results.

### 7.3.4 Experiment 7.4

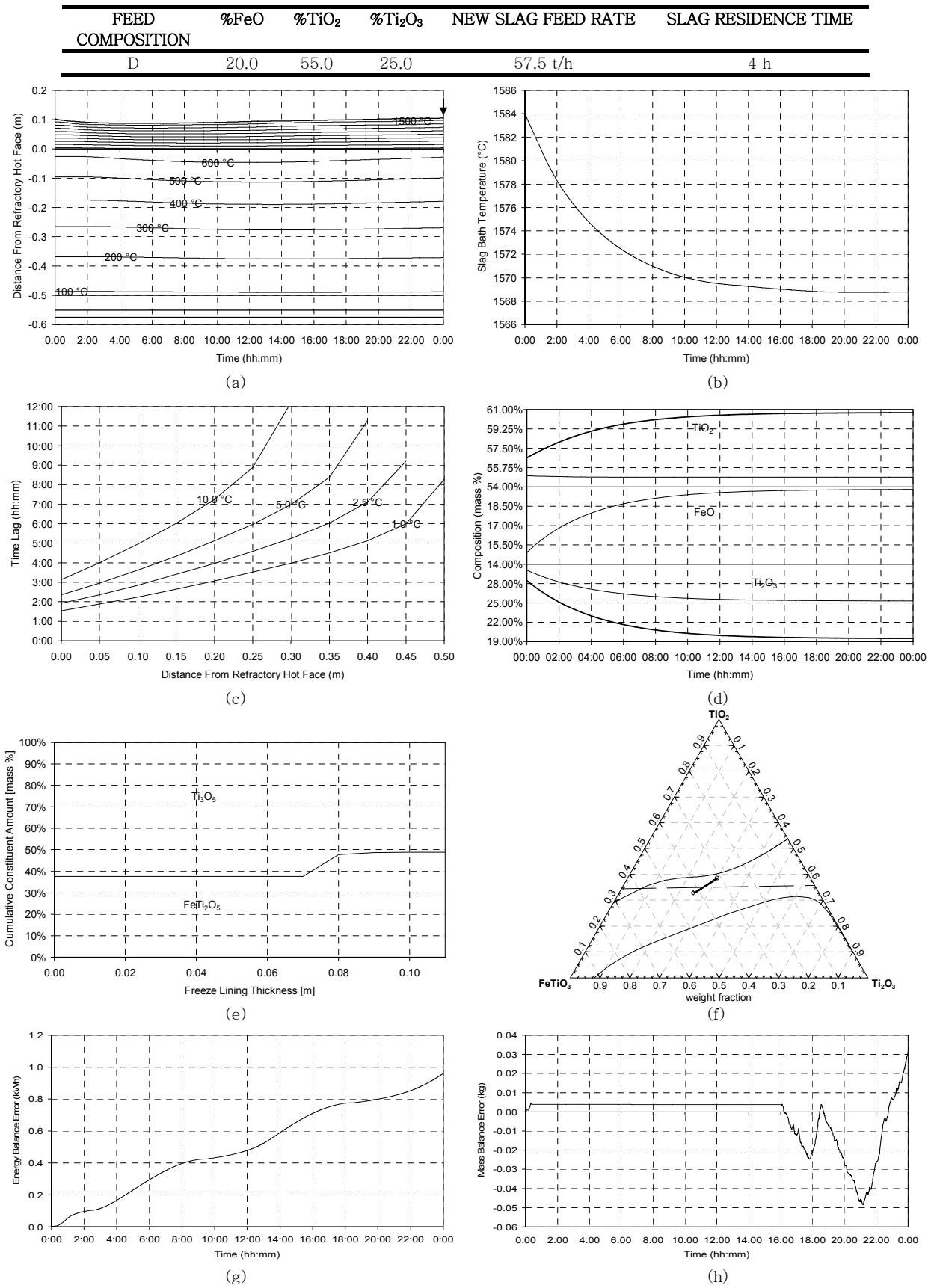


Figure 94 – Experiment 7.4 results.

### 7.3.5 Experiment 7.5

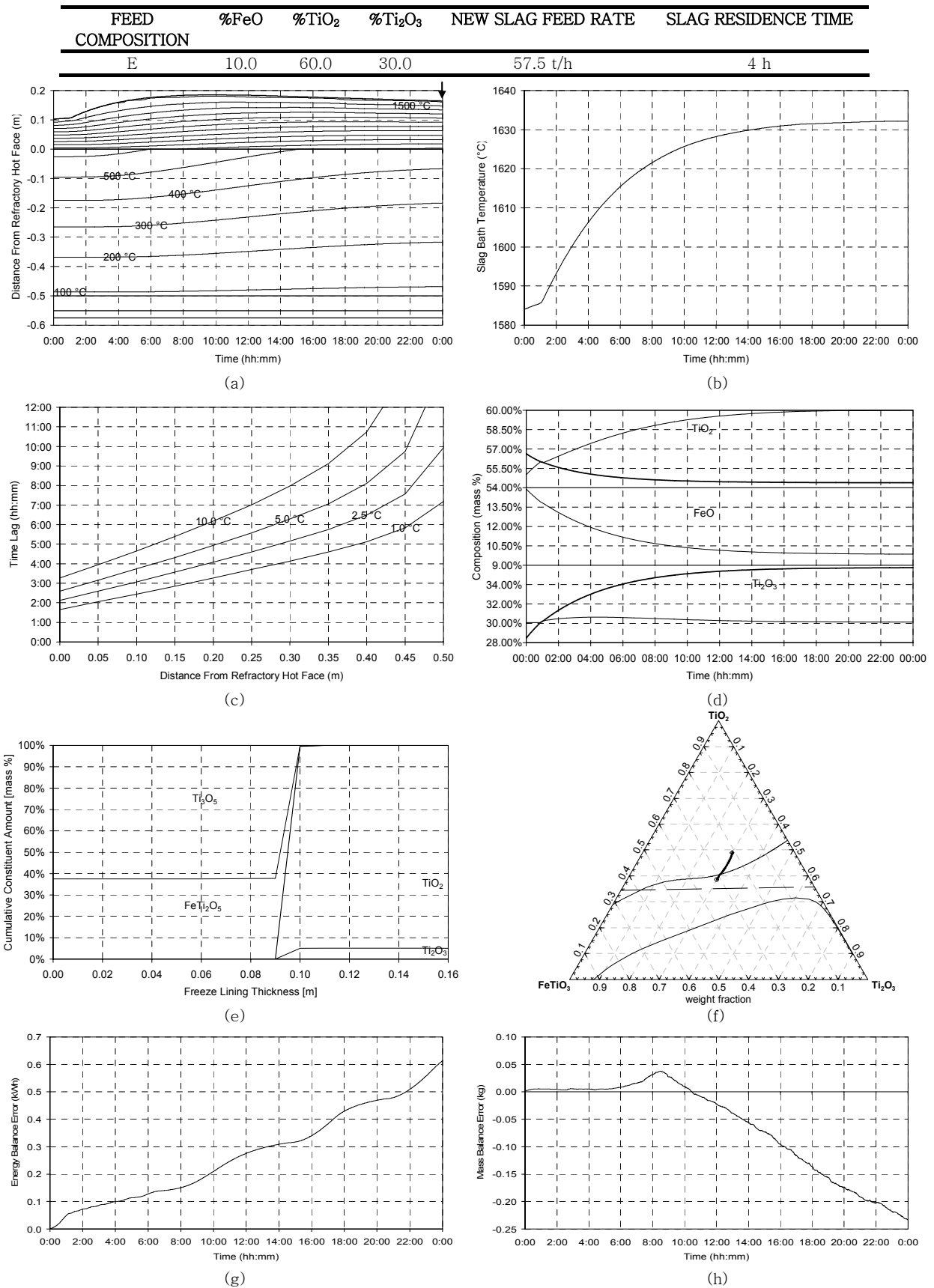


Figure 95 – Experiment 7.5 results.

## 7.3.6 Experiment 7.6

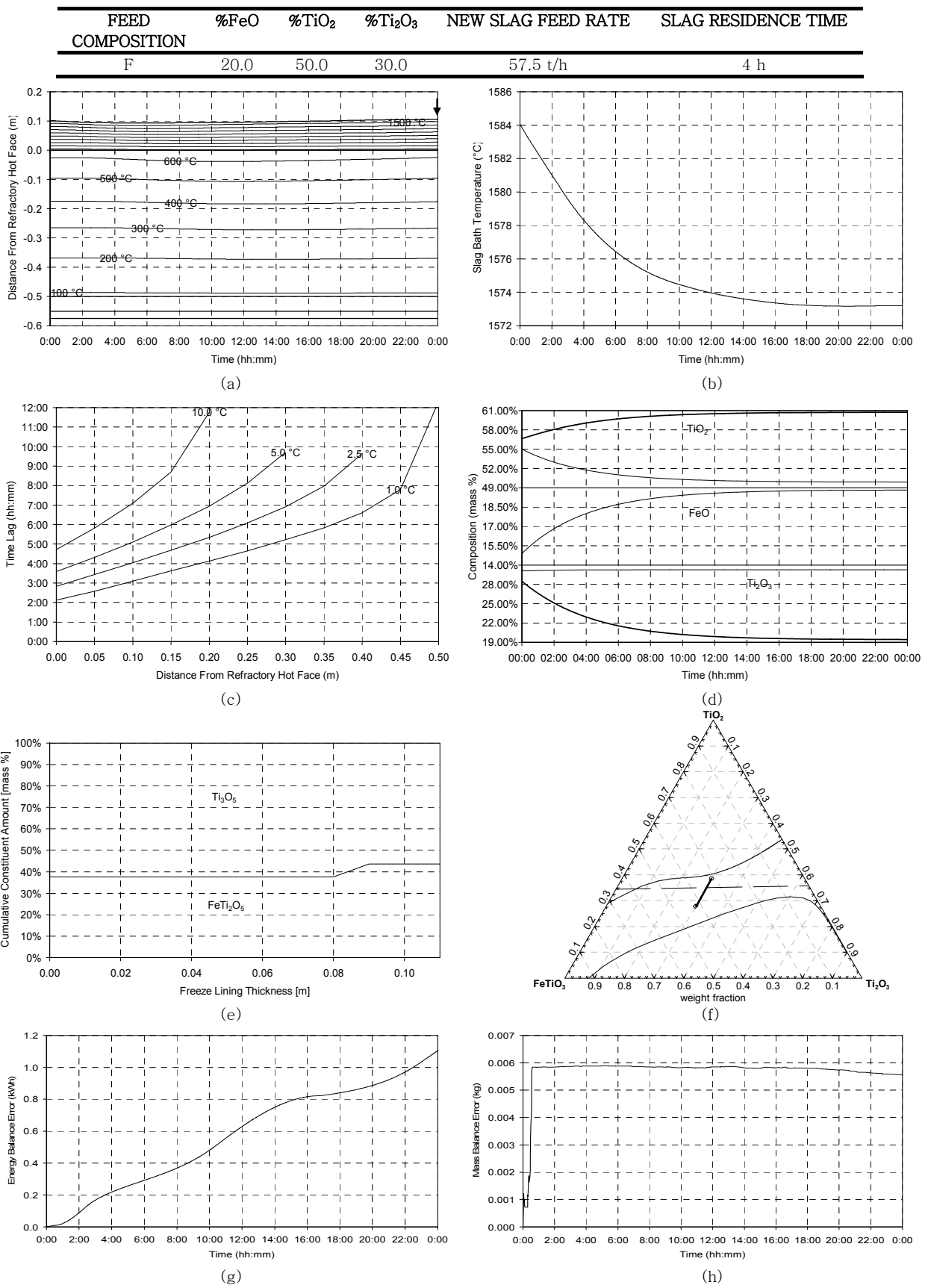


Figure 96 – Experiment 7.6 results.

## 7.3.7 Experiment 7.7

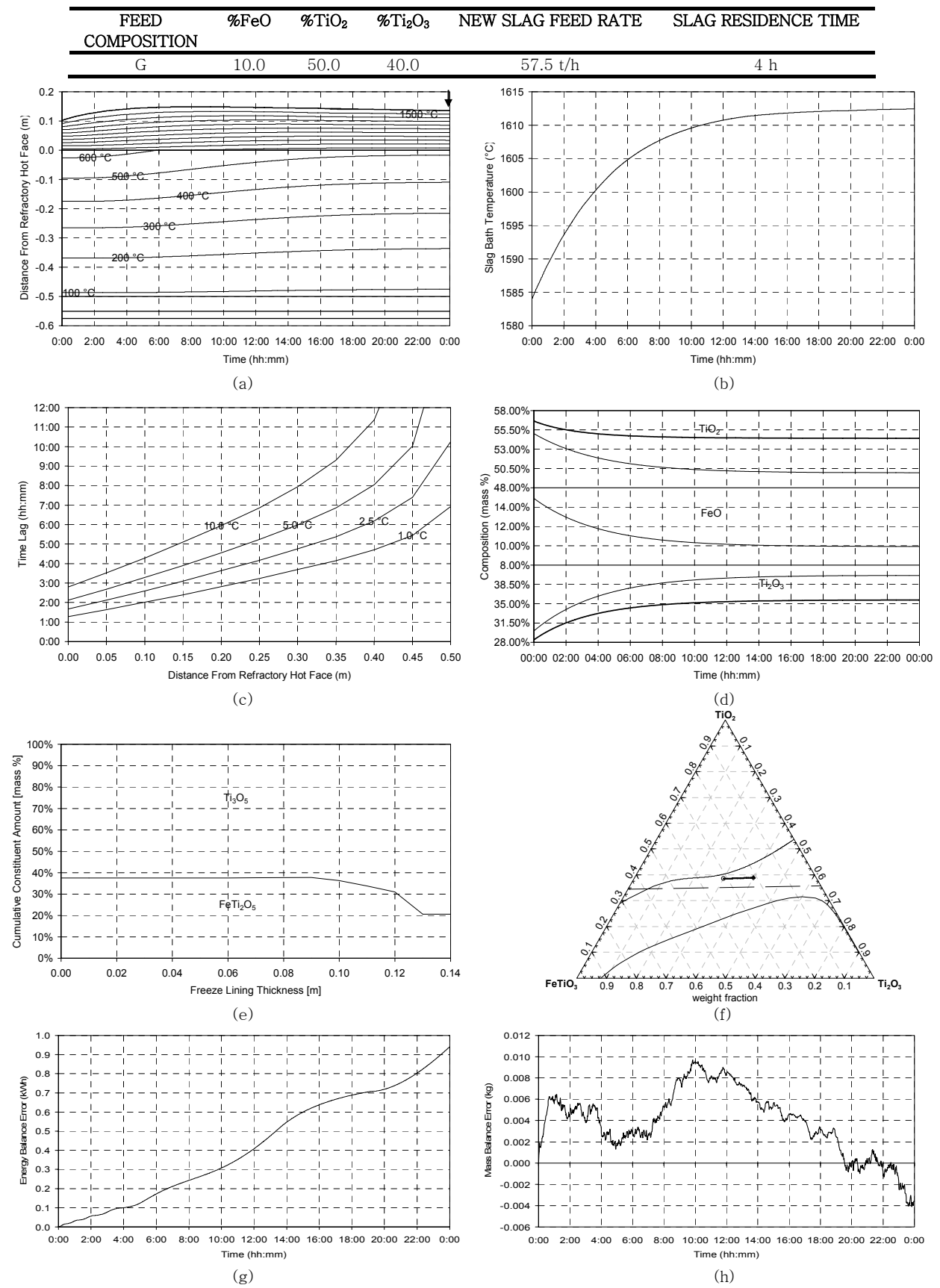


Figure 97 – Experiment 7.7 results.

## 7.3.8 Experiment 7.8

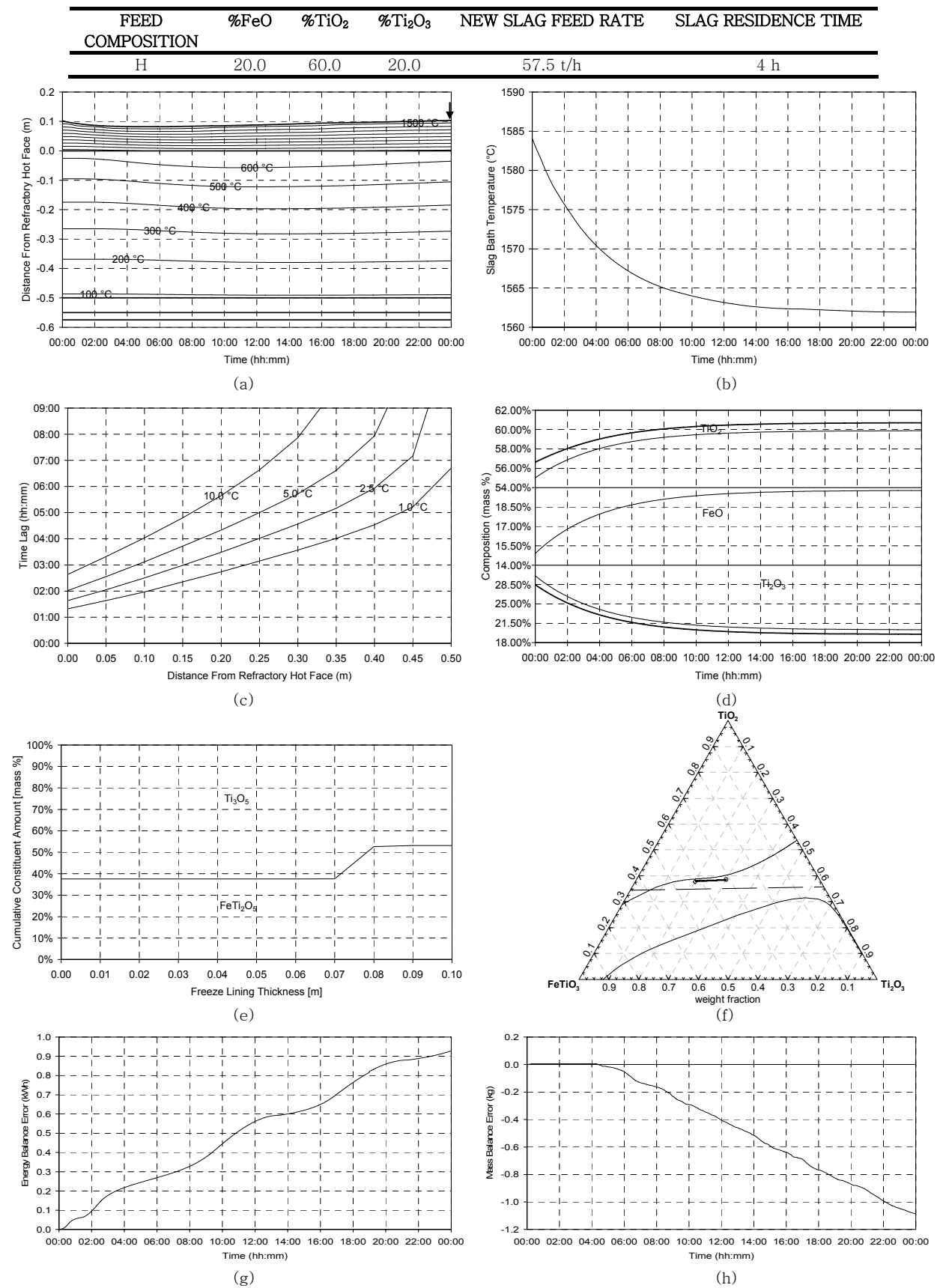


Figure 98 – Experiment 7.8 results.

## 7.3.9 Experiment 7.9

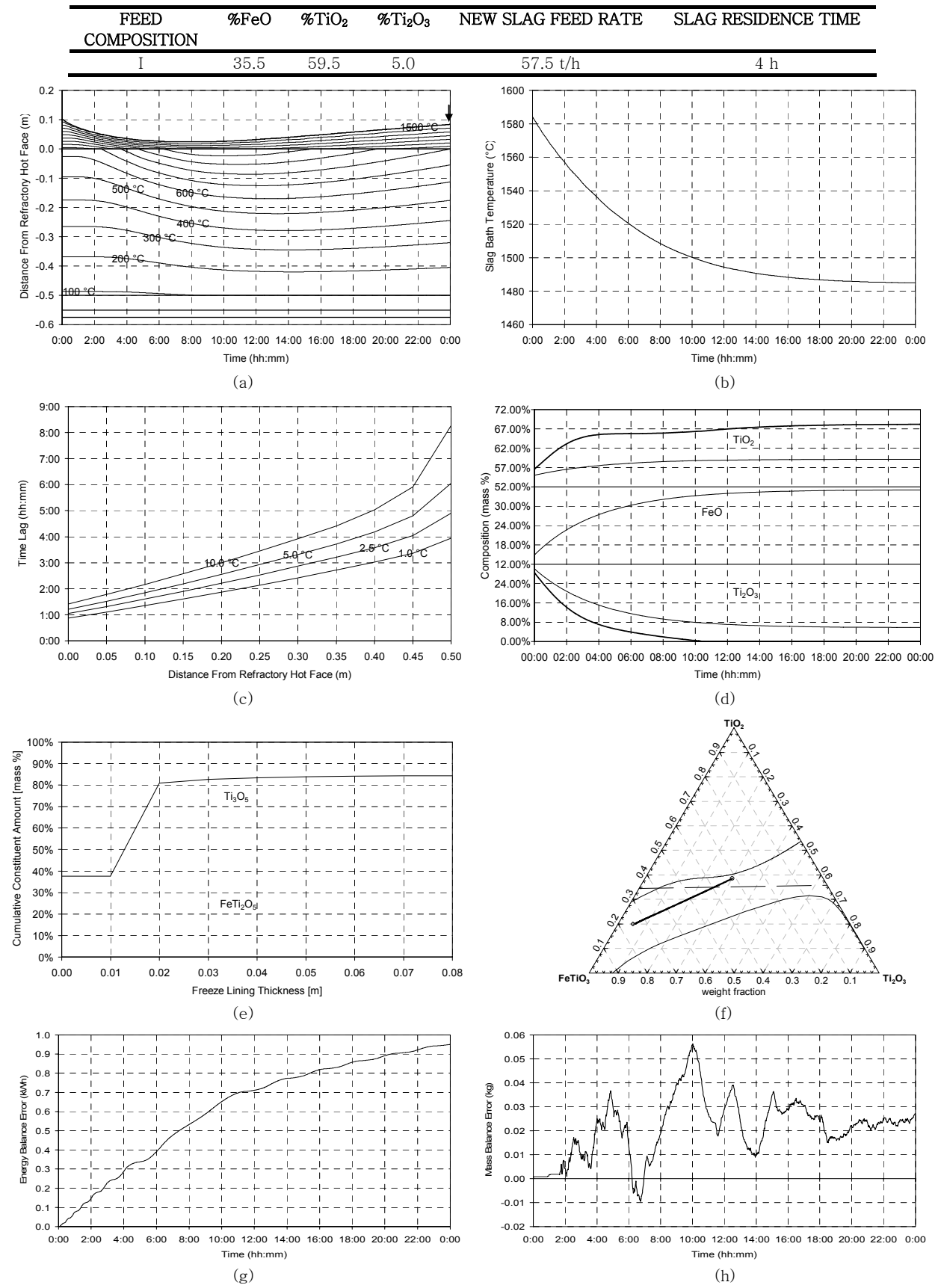


Figure 99 – Experiment 7.9 results.

## 7.3.10 Experiment 7.10

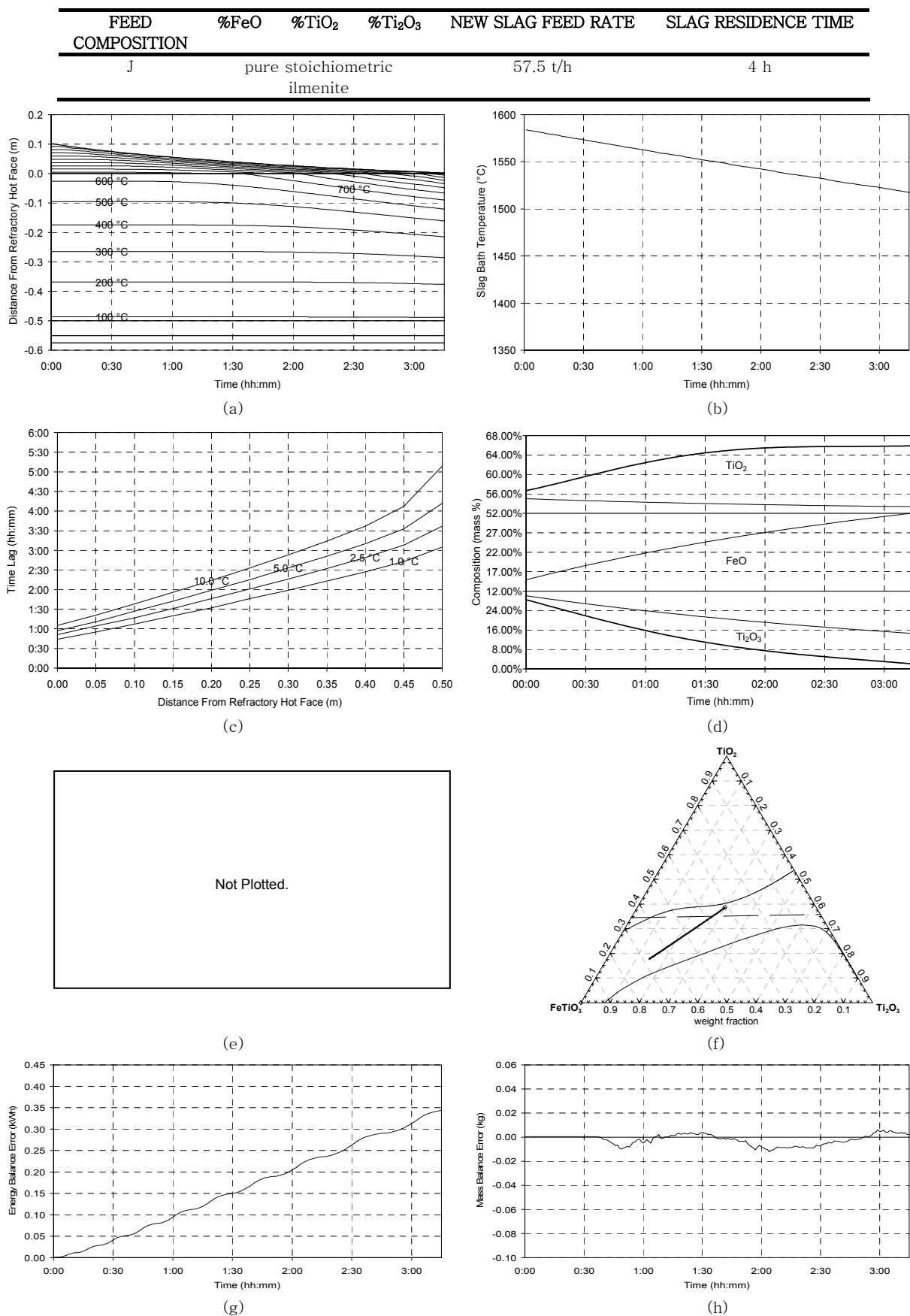


Figure 100 – Experiment 7.10 results.

## 7.3.11 Experiment 7.11

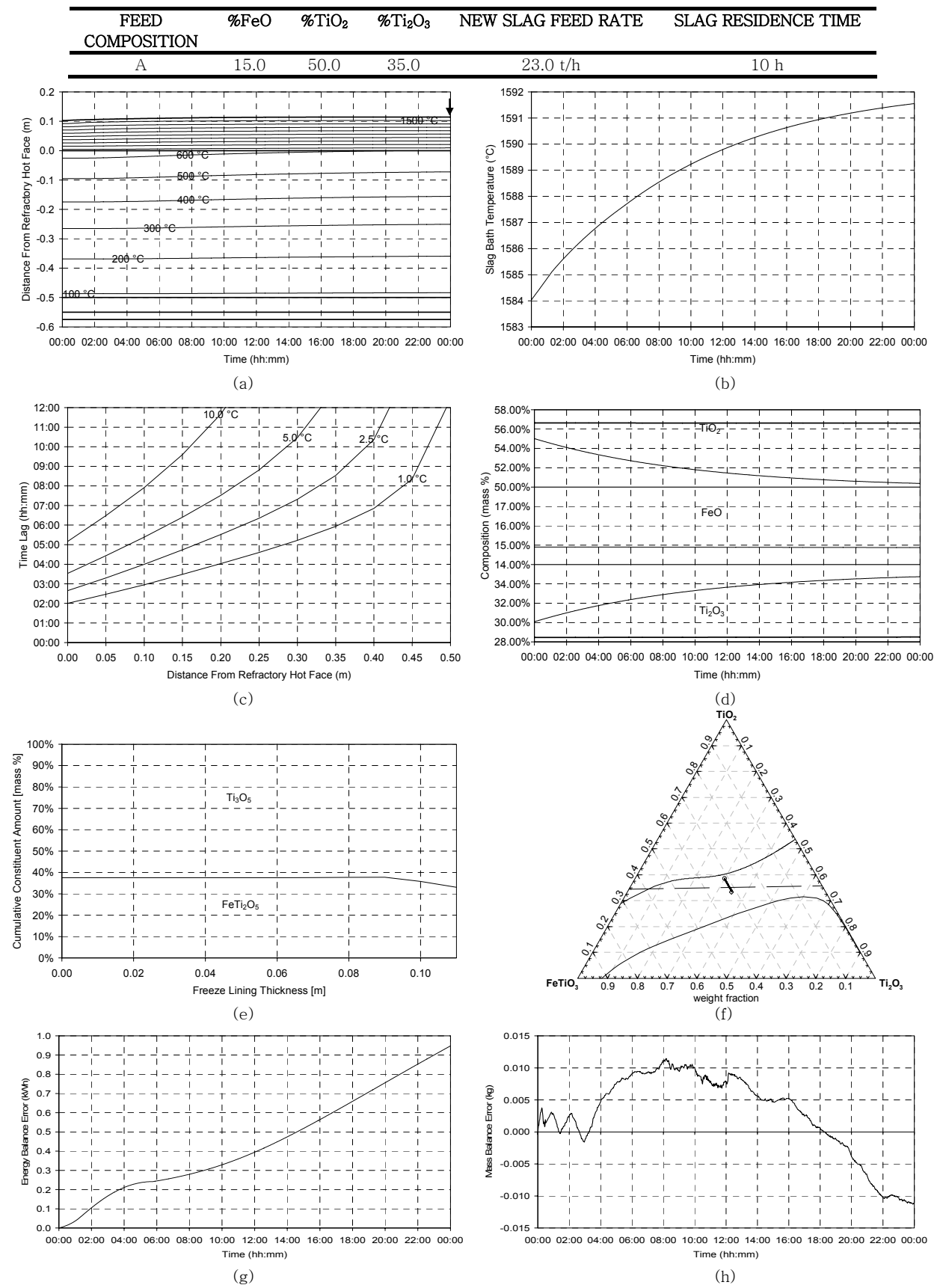


Figure 101 – Experiment 7.11 results.

## 7.3.12 Experiment 7.12

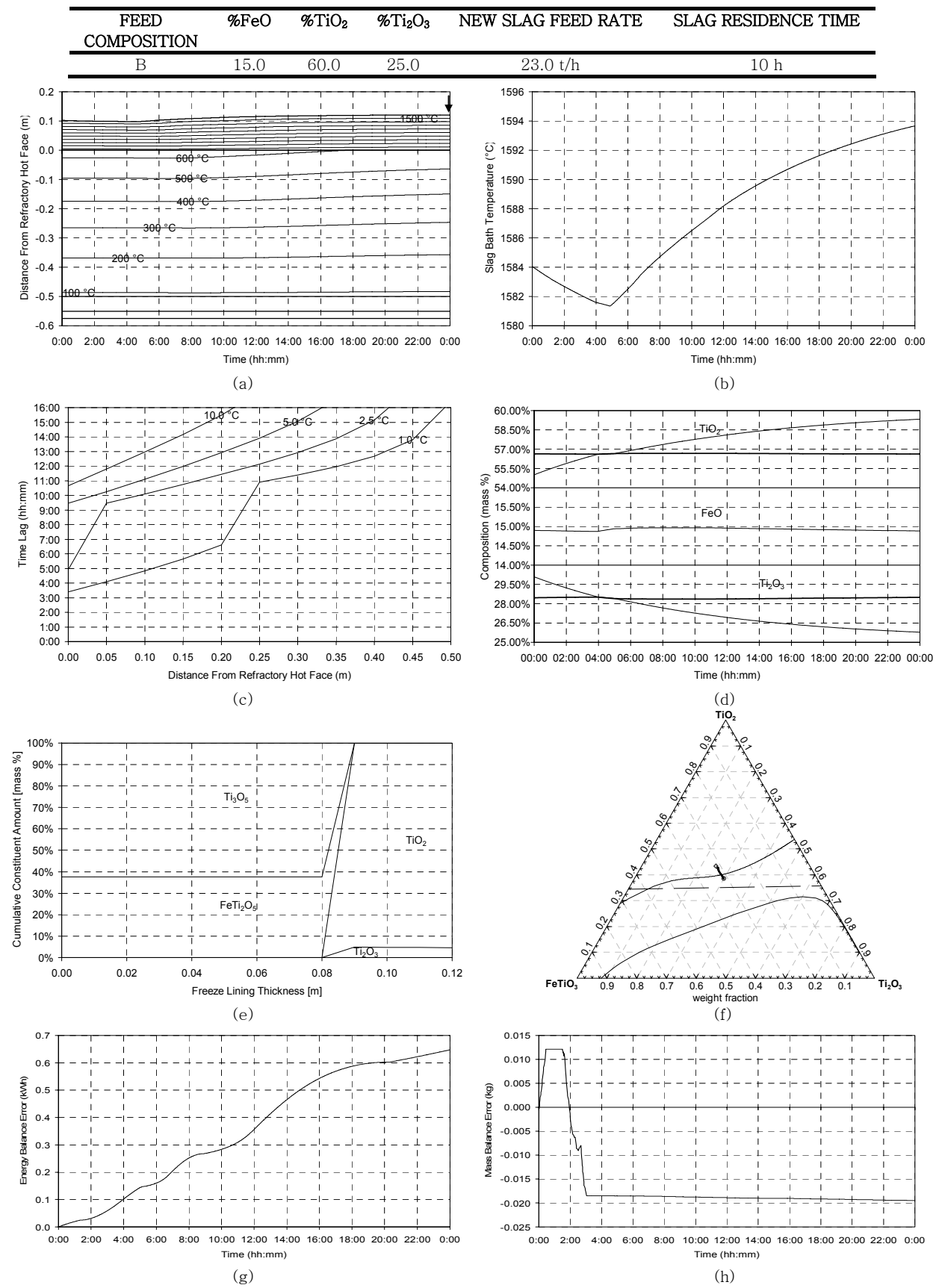


Figure 102 – Experiment 7.12 results.

## 7.3.13 Experiment 7.13

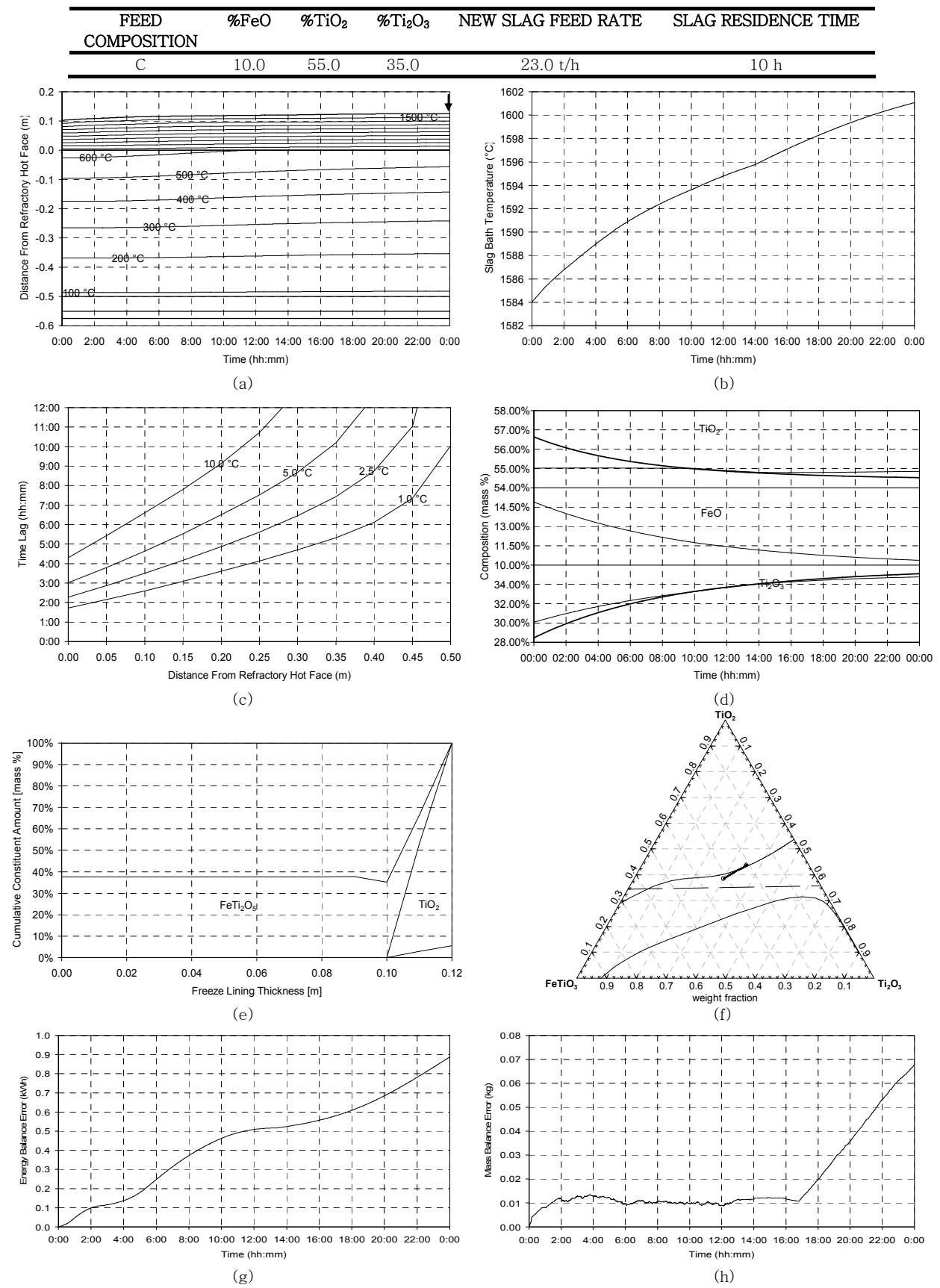


Figure 103 – Experiment 7.13 results.

## 7.3.14 Experiment 7.14

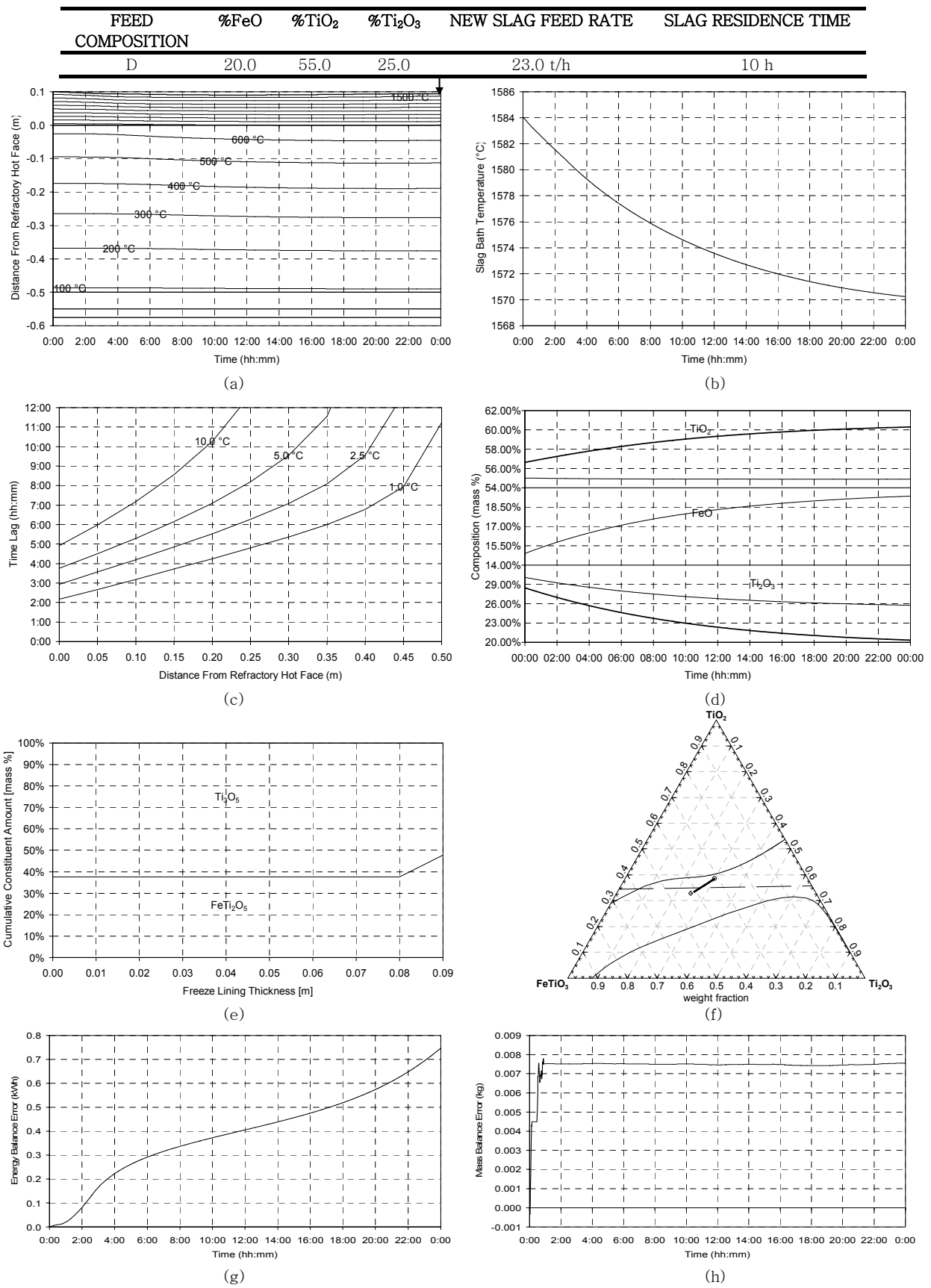


Figure 104 – Experiment 7.14 results.

## 7.3.15 Experiment 7.15

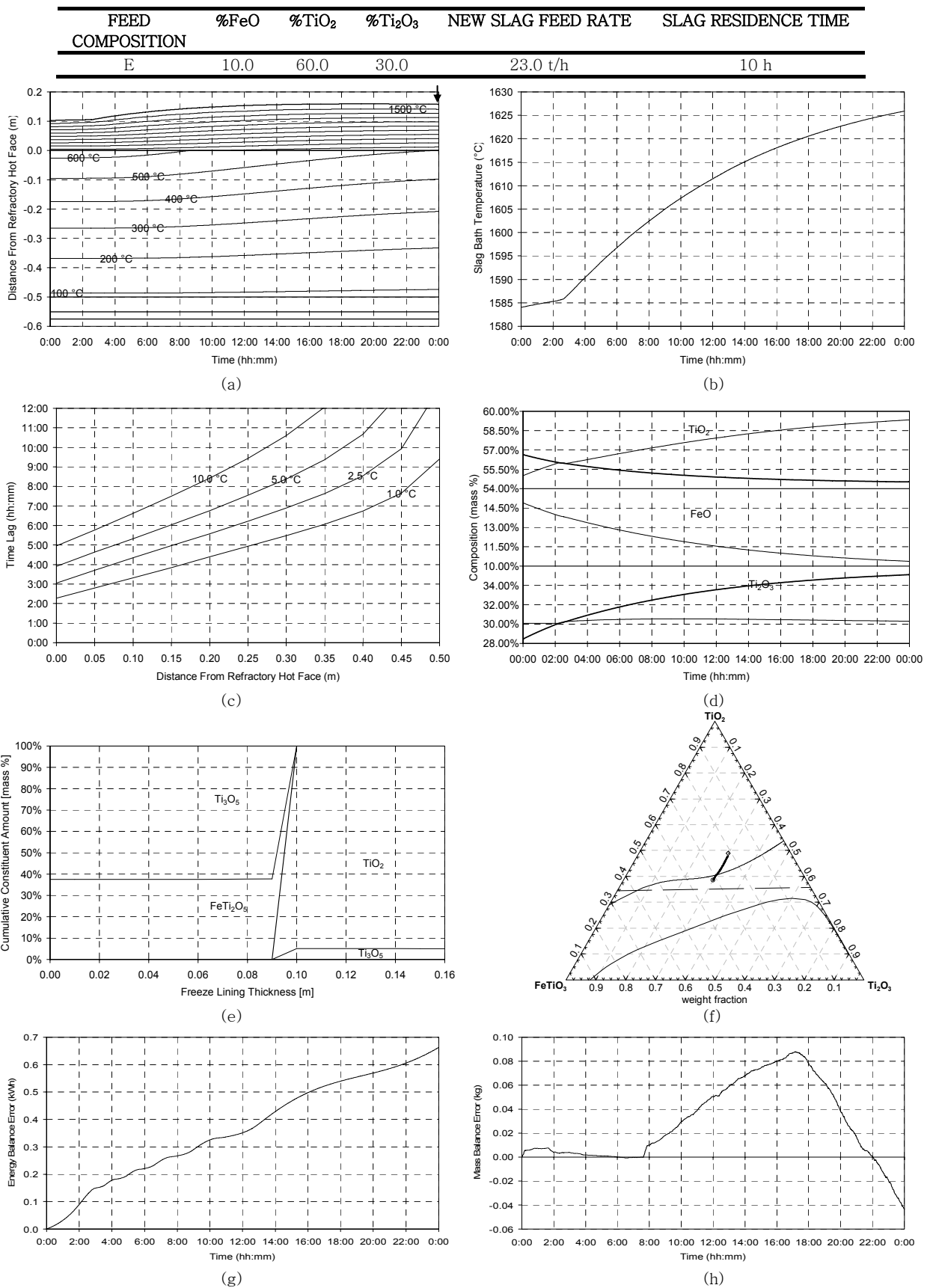


Figure 105 – Experiment 7.15 results.

## 7.3.16 Experiment 7.16

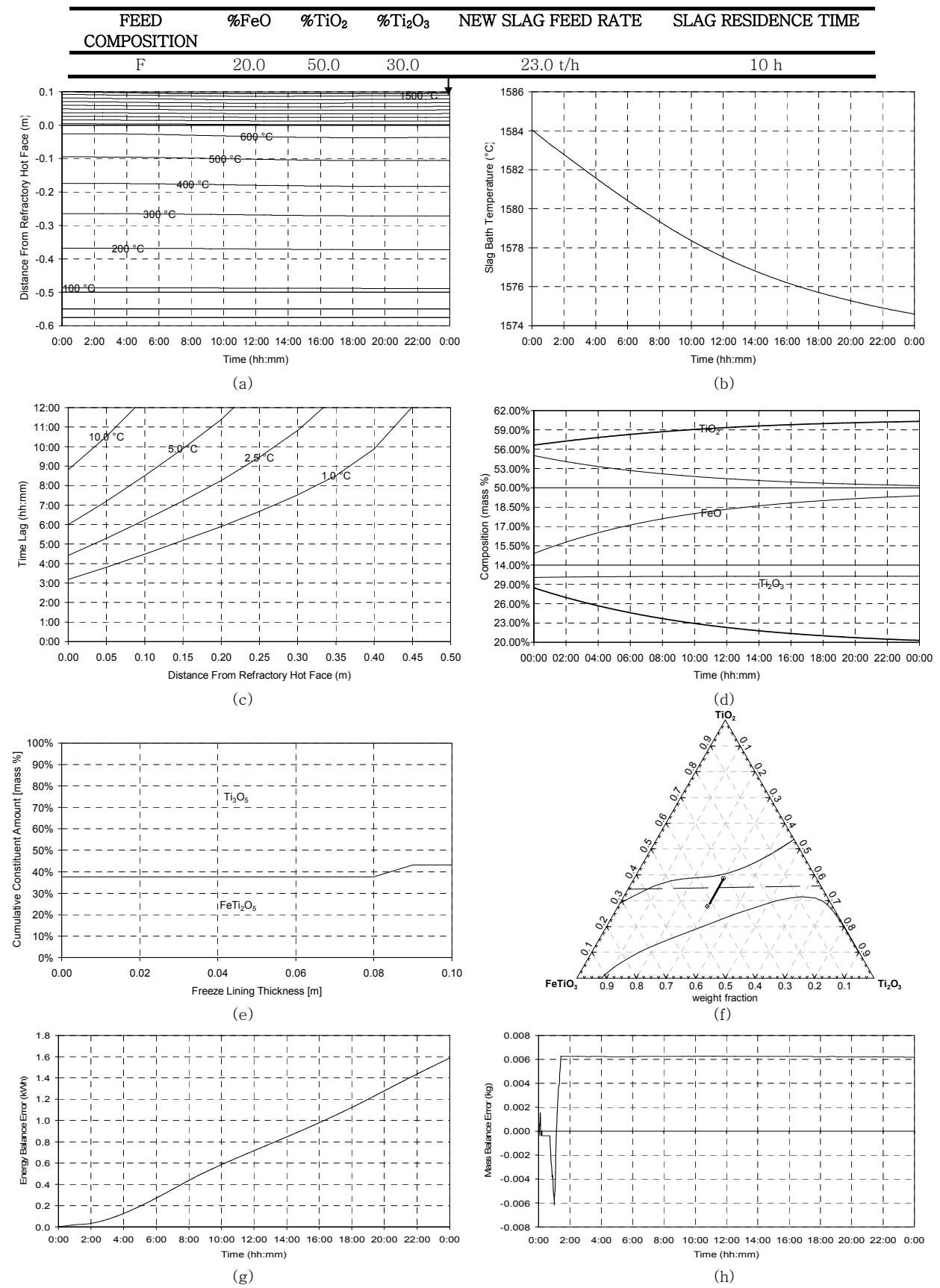


Figure 106 – Experiment 7.16 results.

## 7.3.17 Experiment 7.17

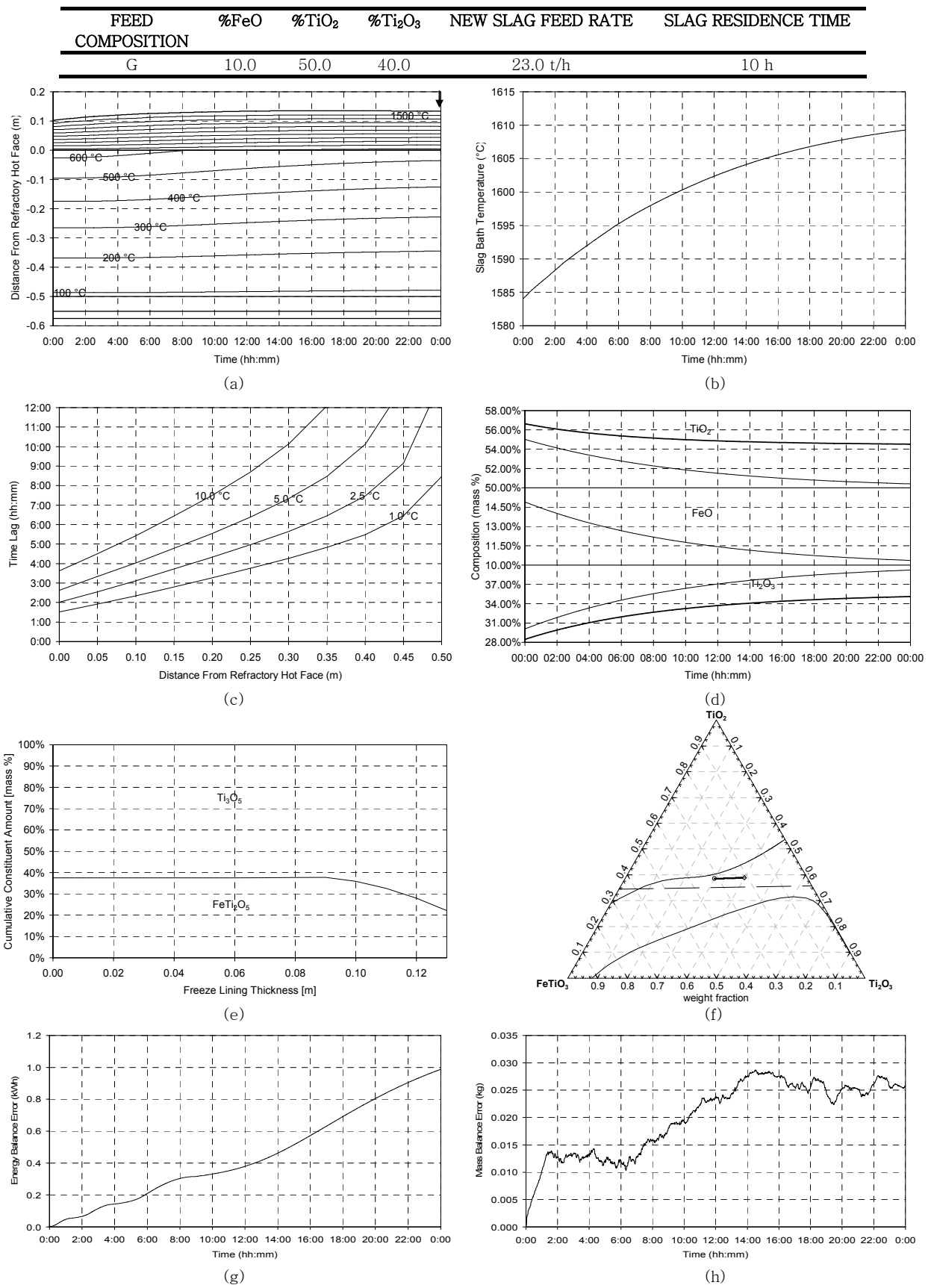


Figure 107 – Experiment 7.17 results.

## 7.3.18 Experiment 7.18

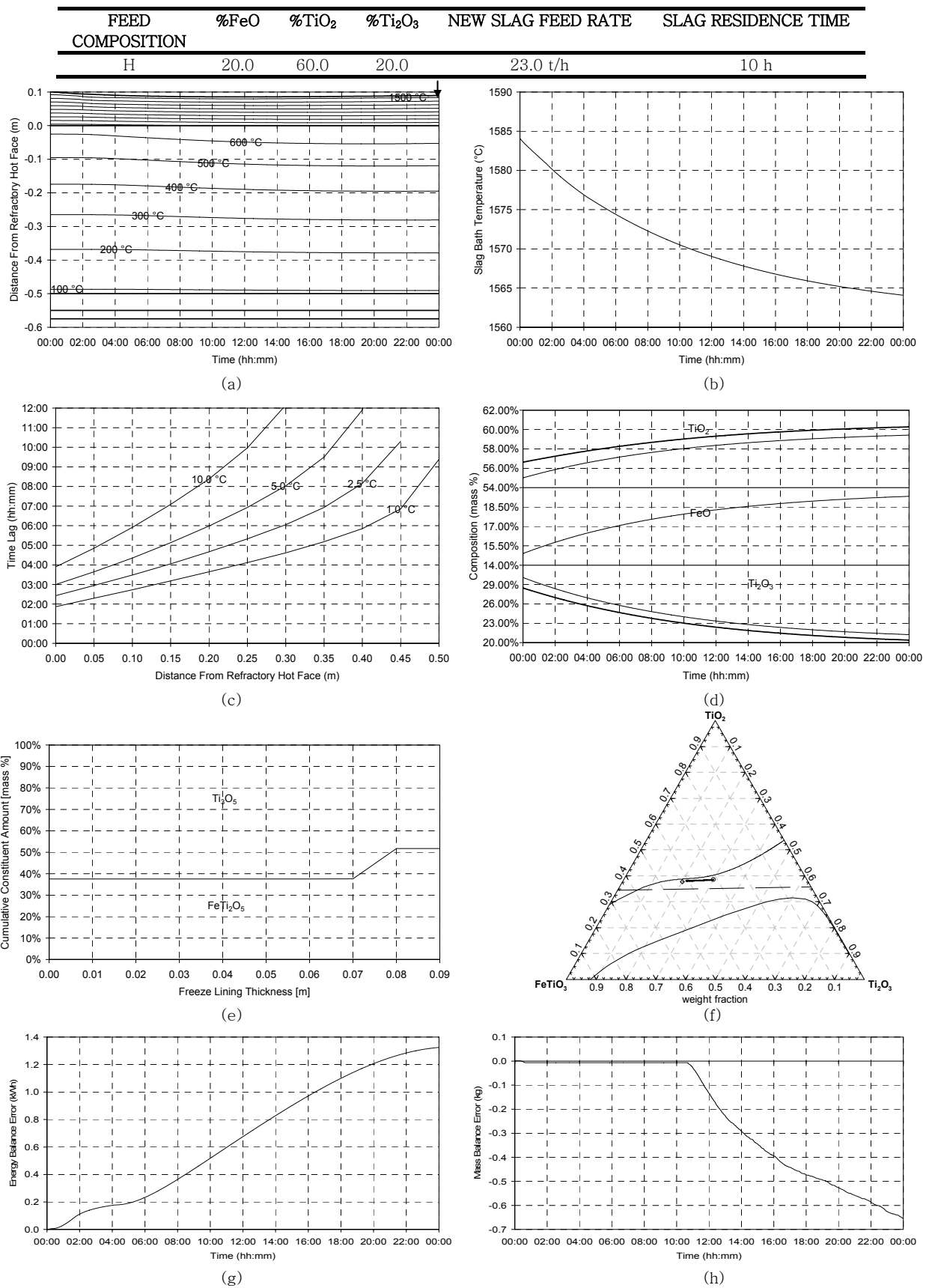


Figure 108 – Experiment 7.18 results.

## 7.3.19 Experiment 7.19

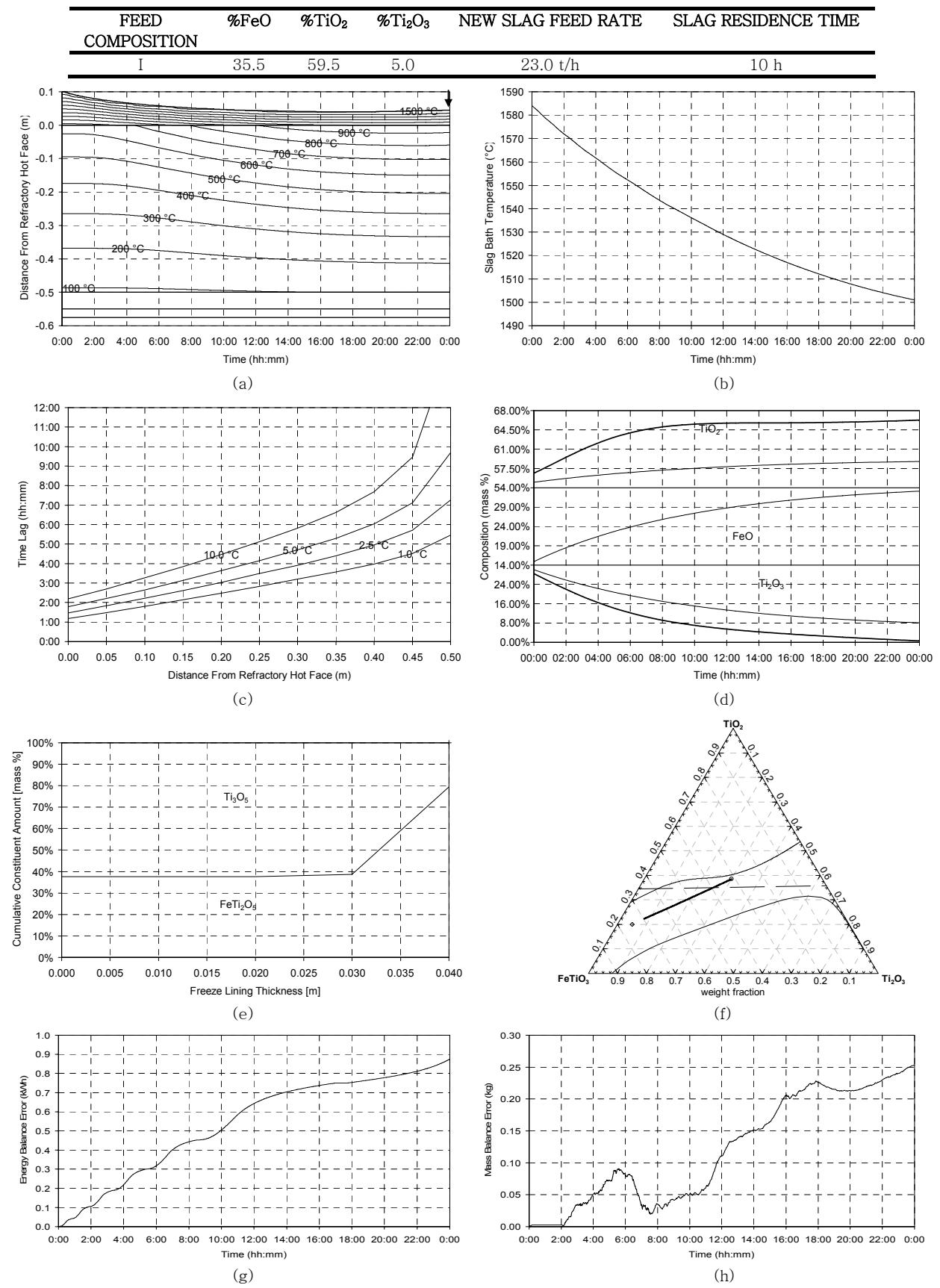


Figure 109 – Experiment 7.19 results.

## 7.3.20 Experiment 7.20

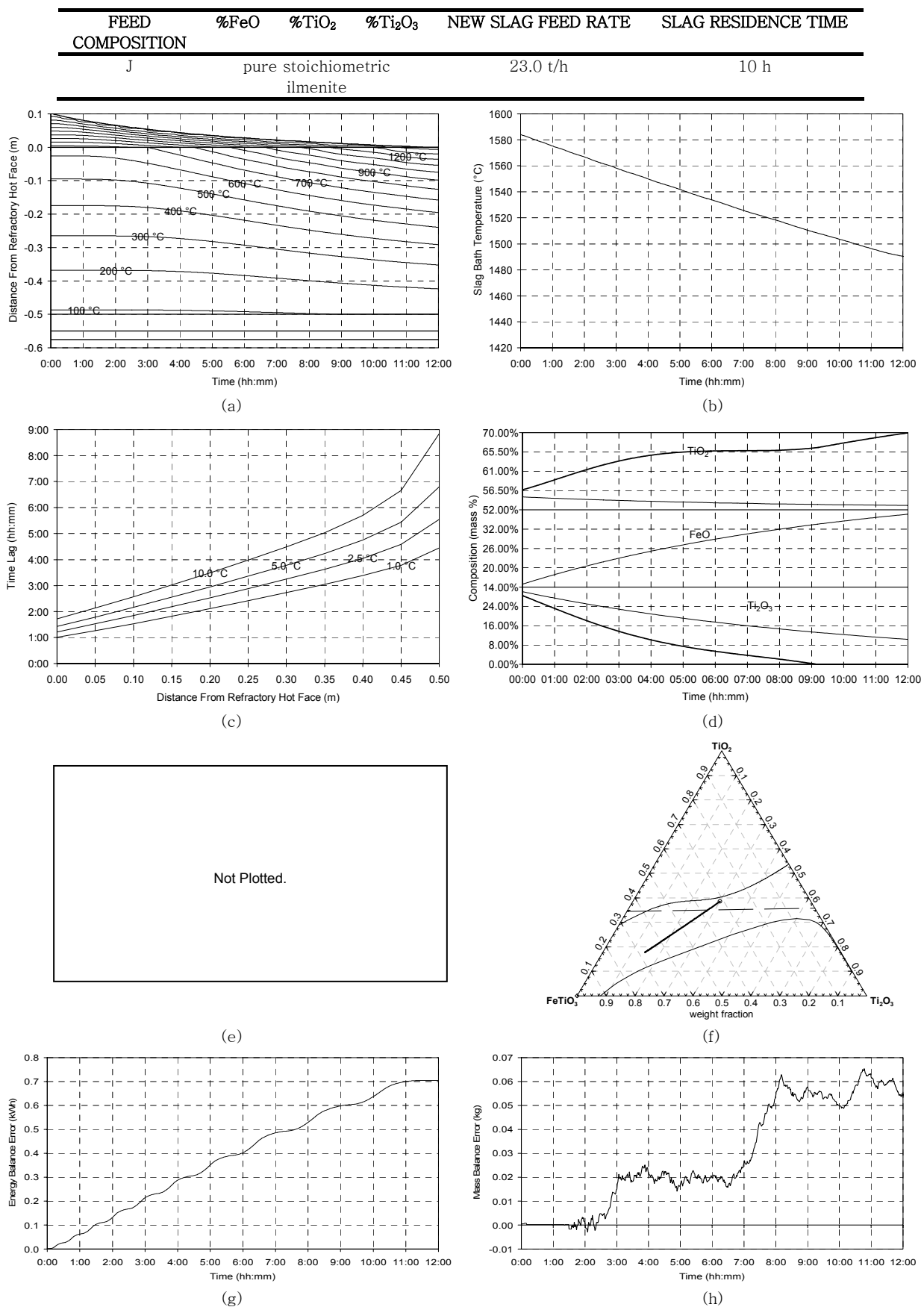


Figure 110 – Experiment 7.20 results.

## 7.3.21 Experiment 7.21

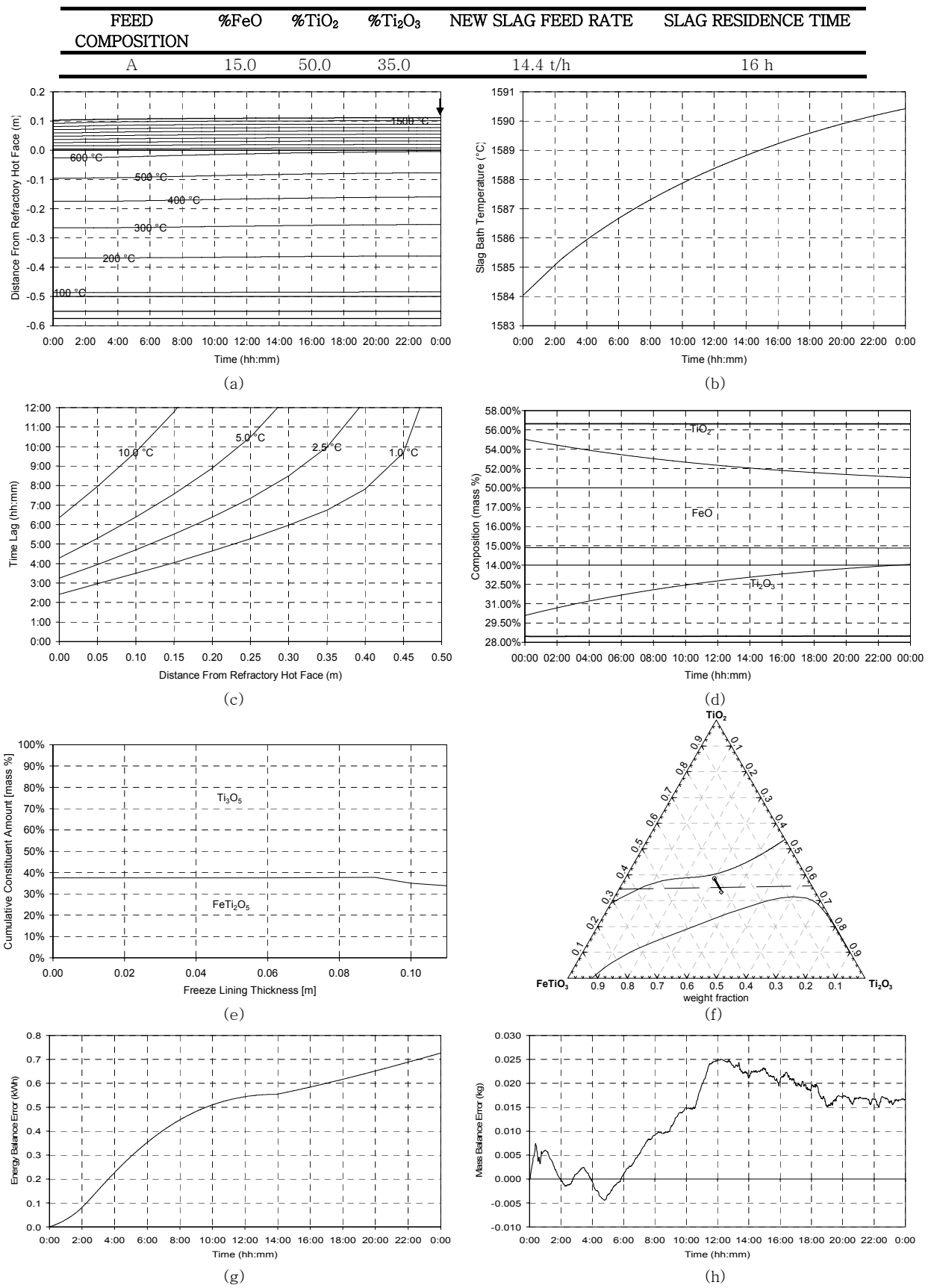


Figure 111 – Experiment 7.21 results.

## 7.3.22 Experiment 7.22

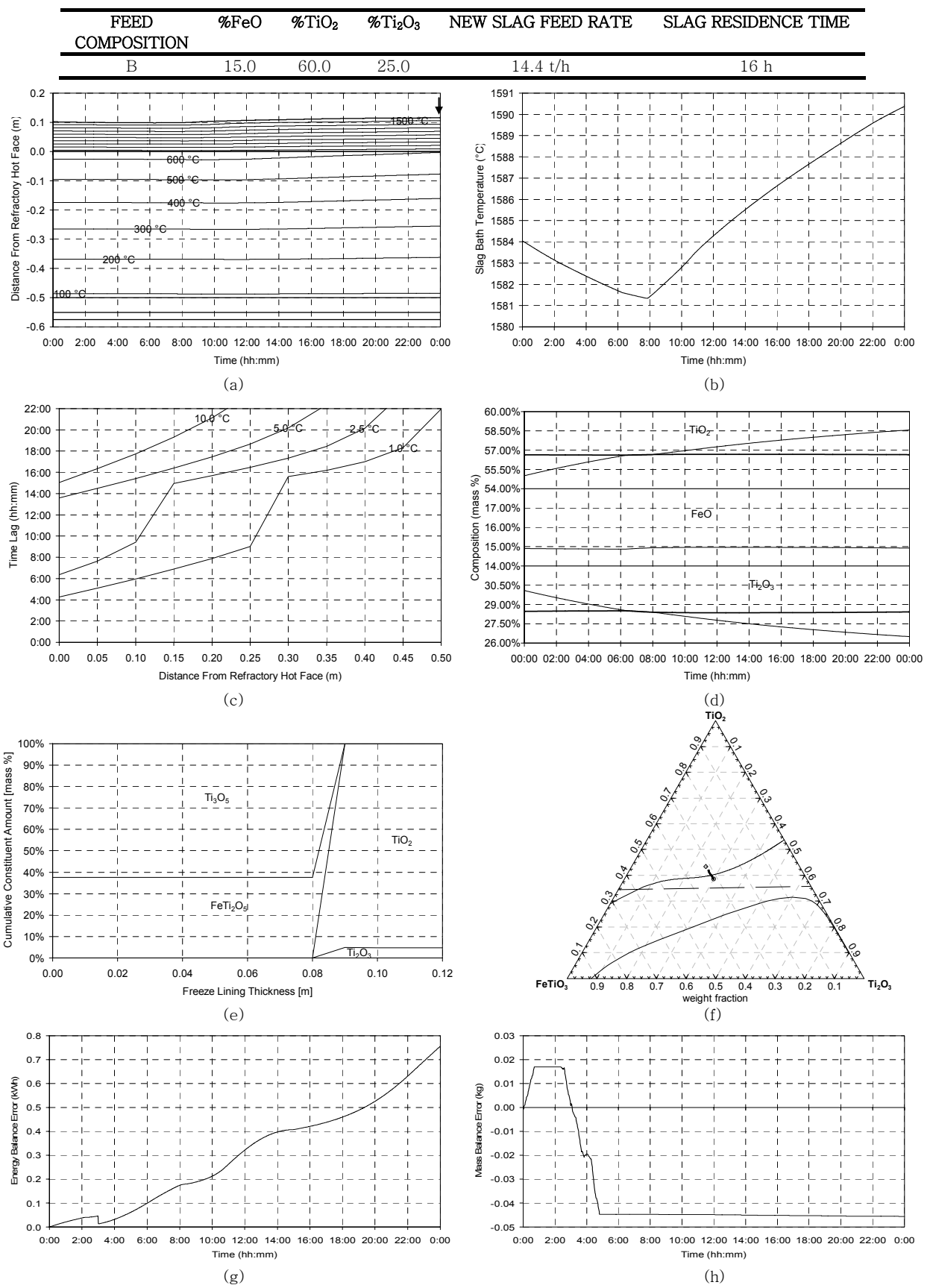


Figure 112 – Experiment 7.22 results.

## 7.3.23 Experiment 7.23

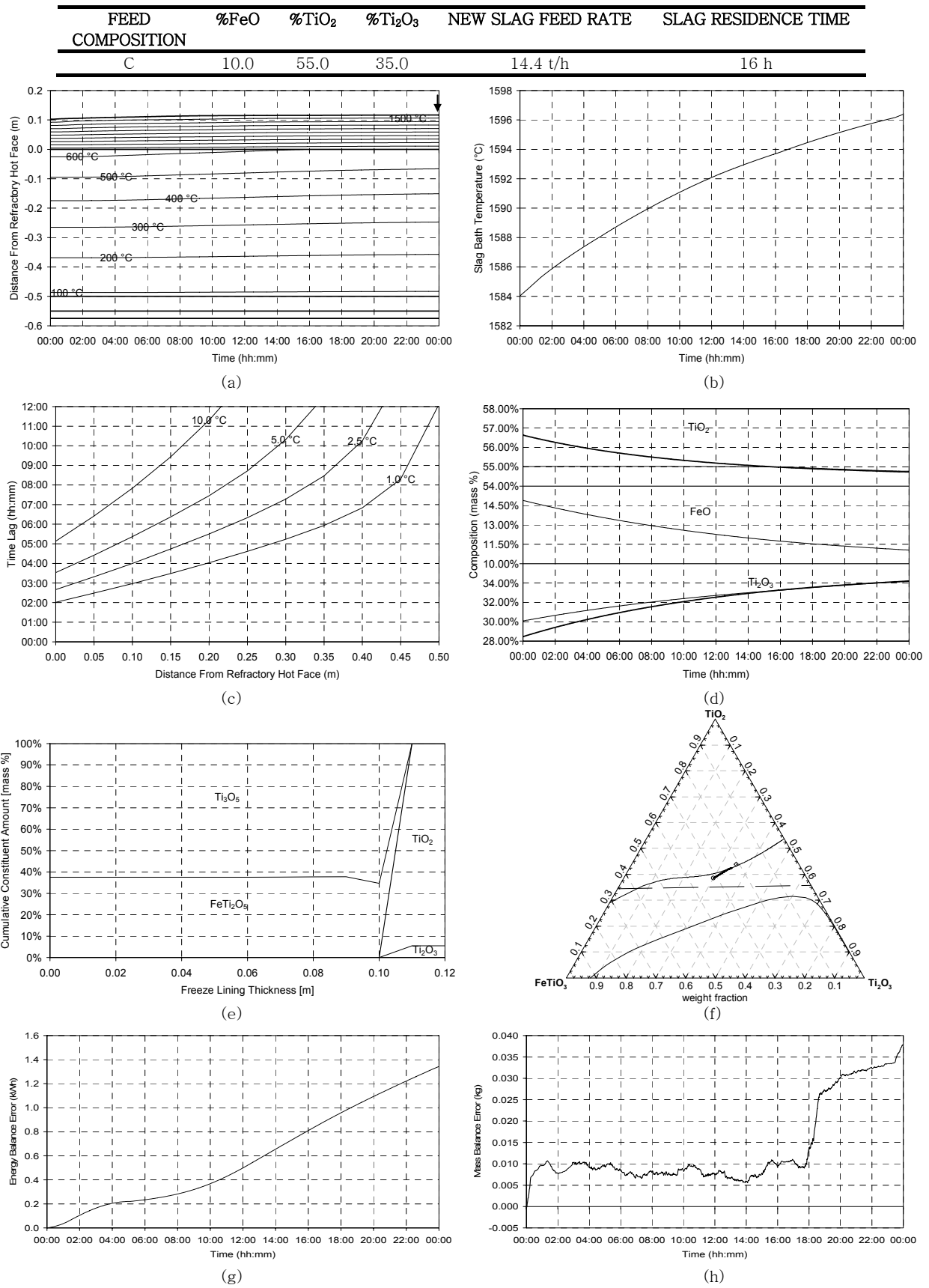


Figure 113 – Experiment 7.23 results.

## 7.3.24 Experiment 7.24

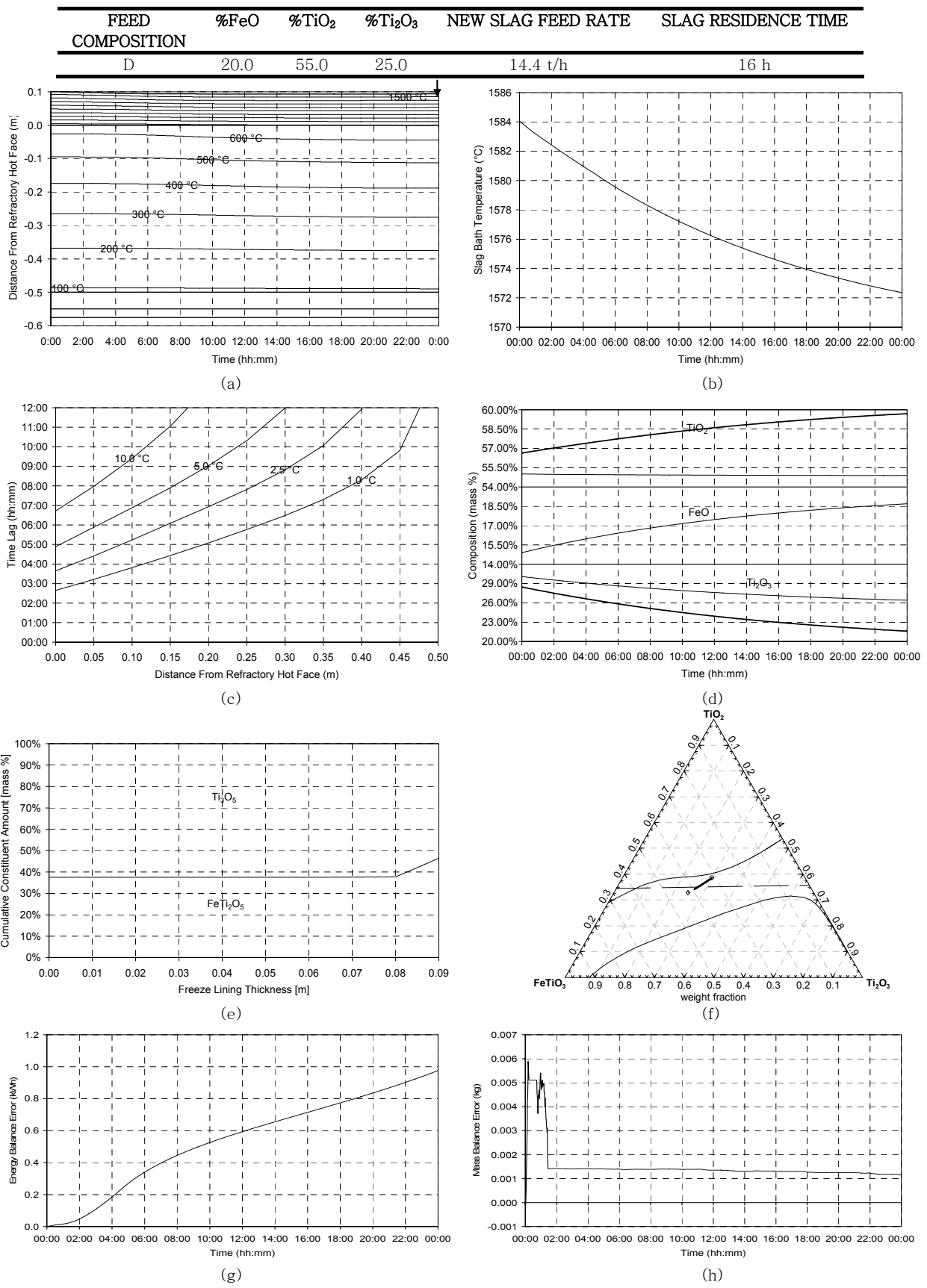


Figure 114 – Experiment 7.24 results.

## 7.3.25 Experiment 7.25

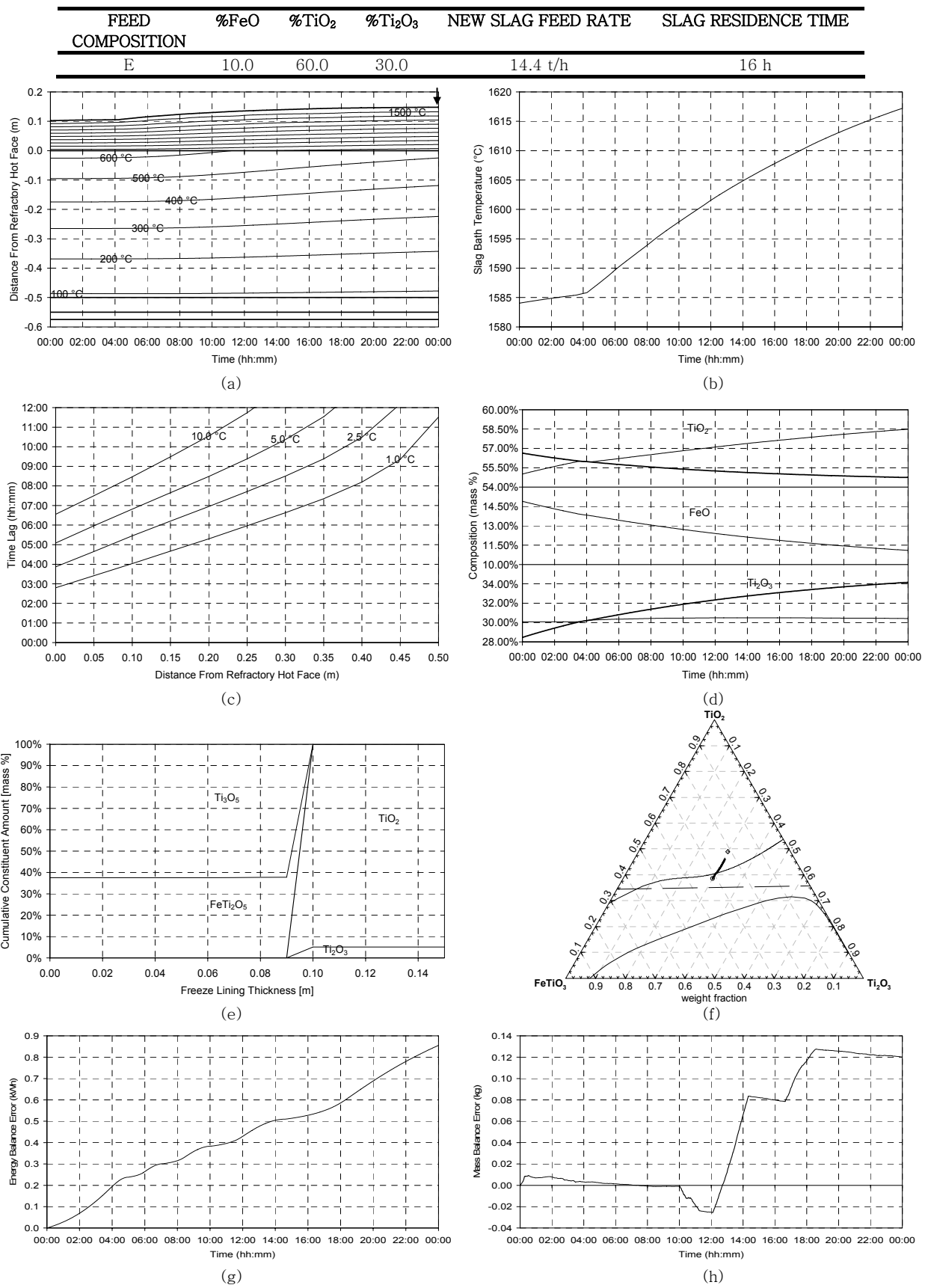


Figure 115 – Experiment 7.25 results.

## 7.3.26 Experiment 7.26

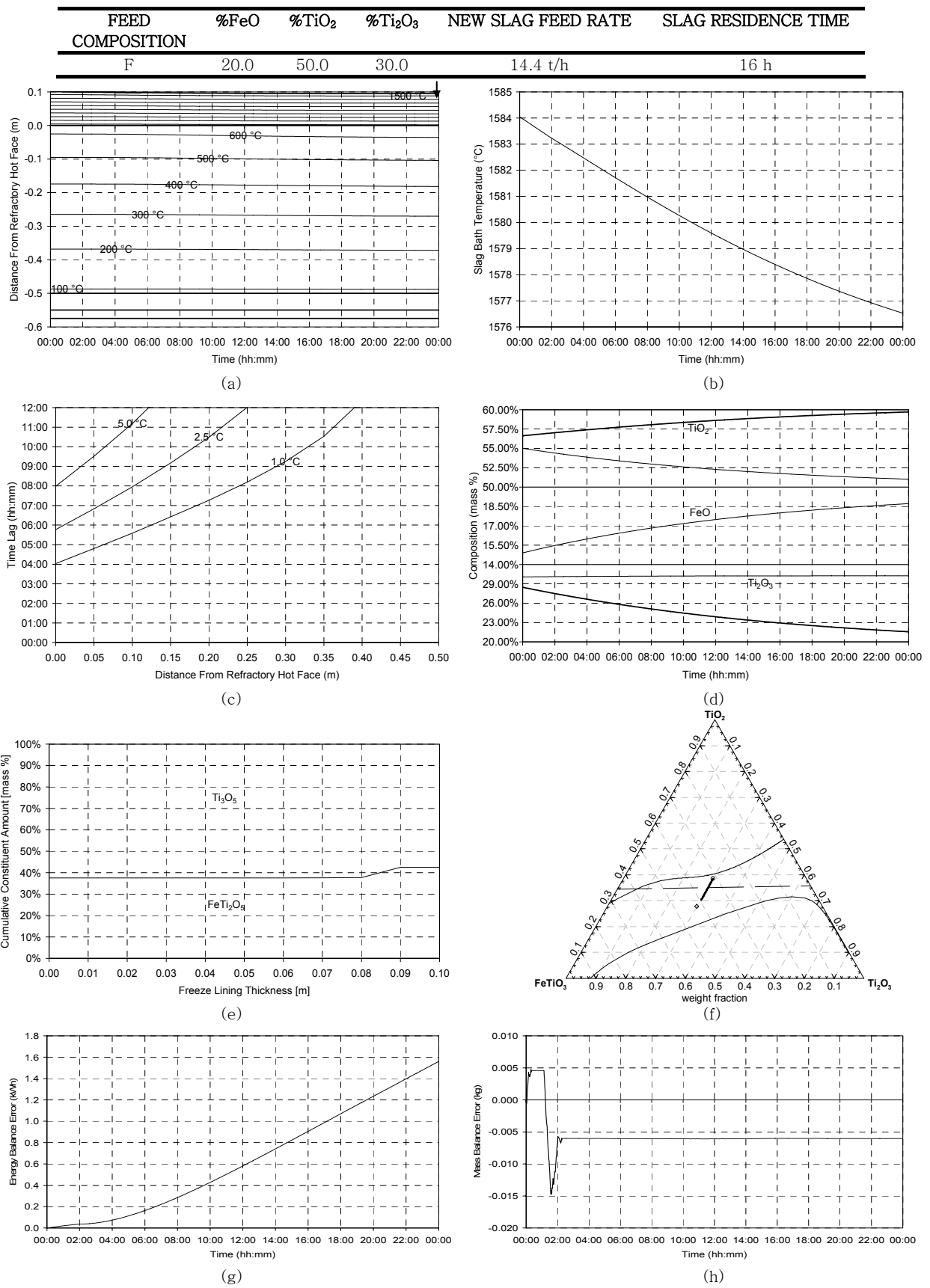


Figure 116 – Experiment 7.26 results.

## 7.3.27 Experiment 7.27

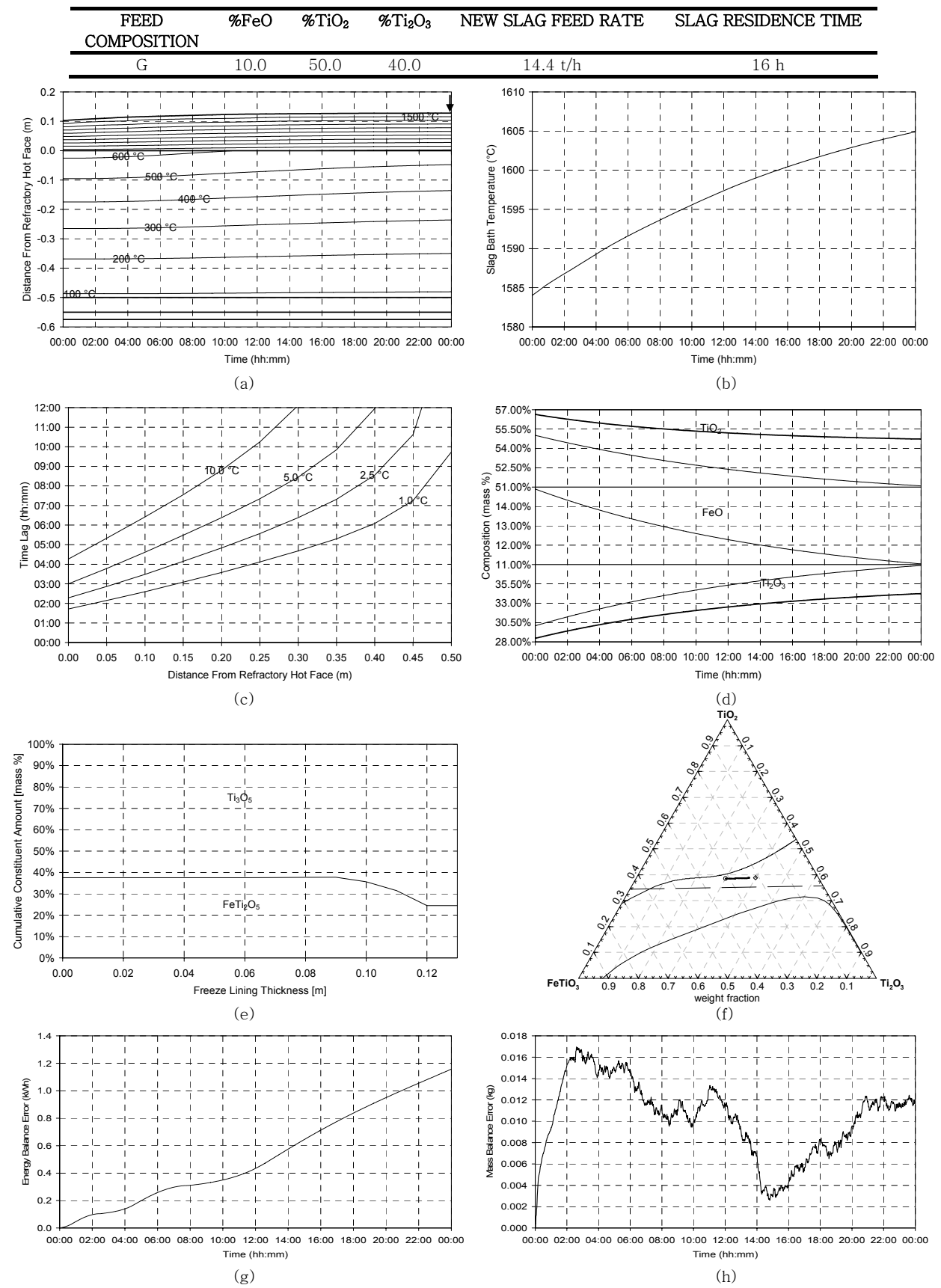


Figure 117 – Experiment 7.27 results.

## 7.3.28 Experiment 7.28

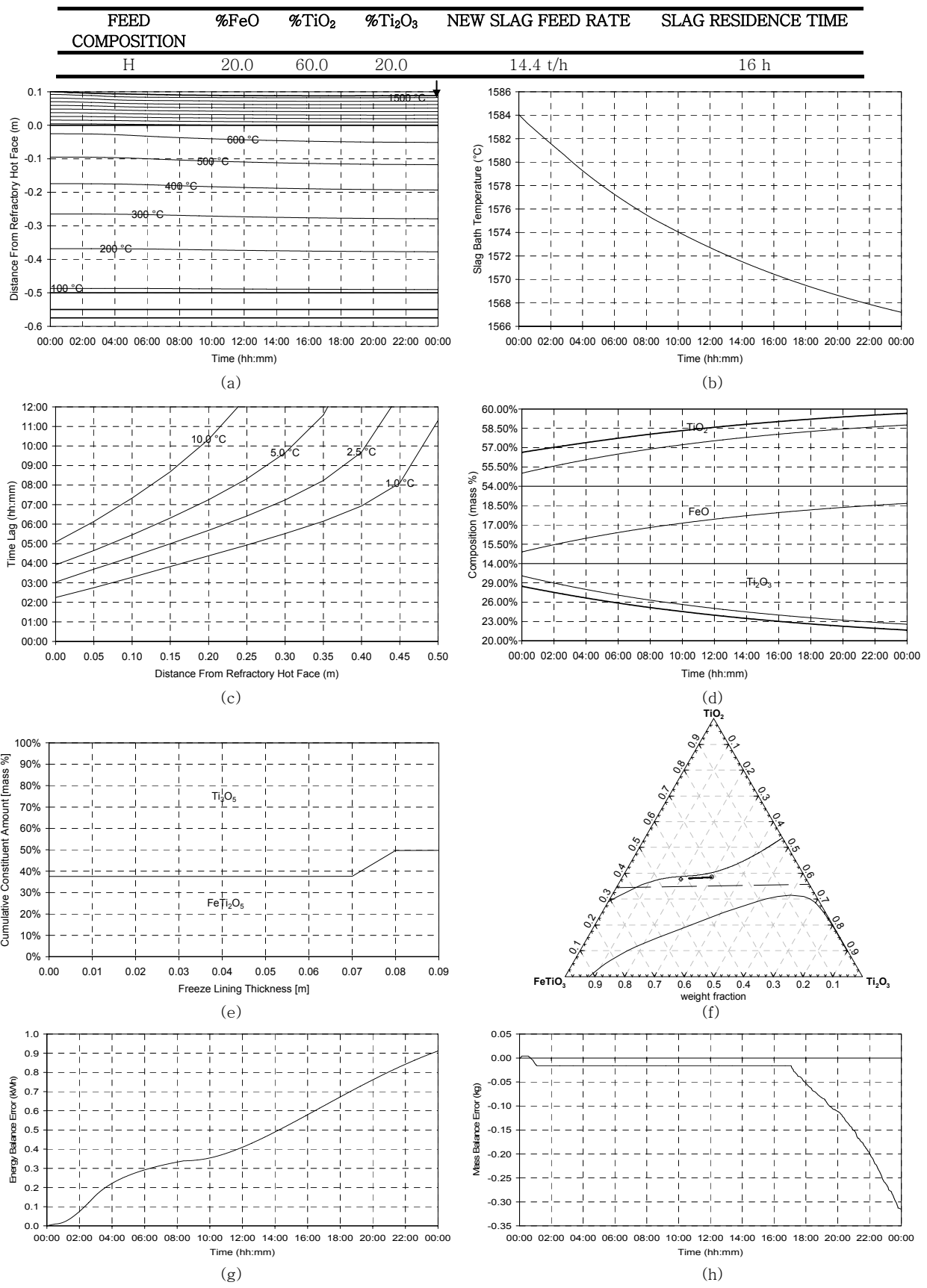


Figure 118 – Experiment 7.28 results.

## 7.3.29 Experiment 7.29

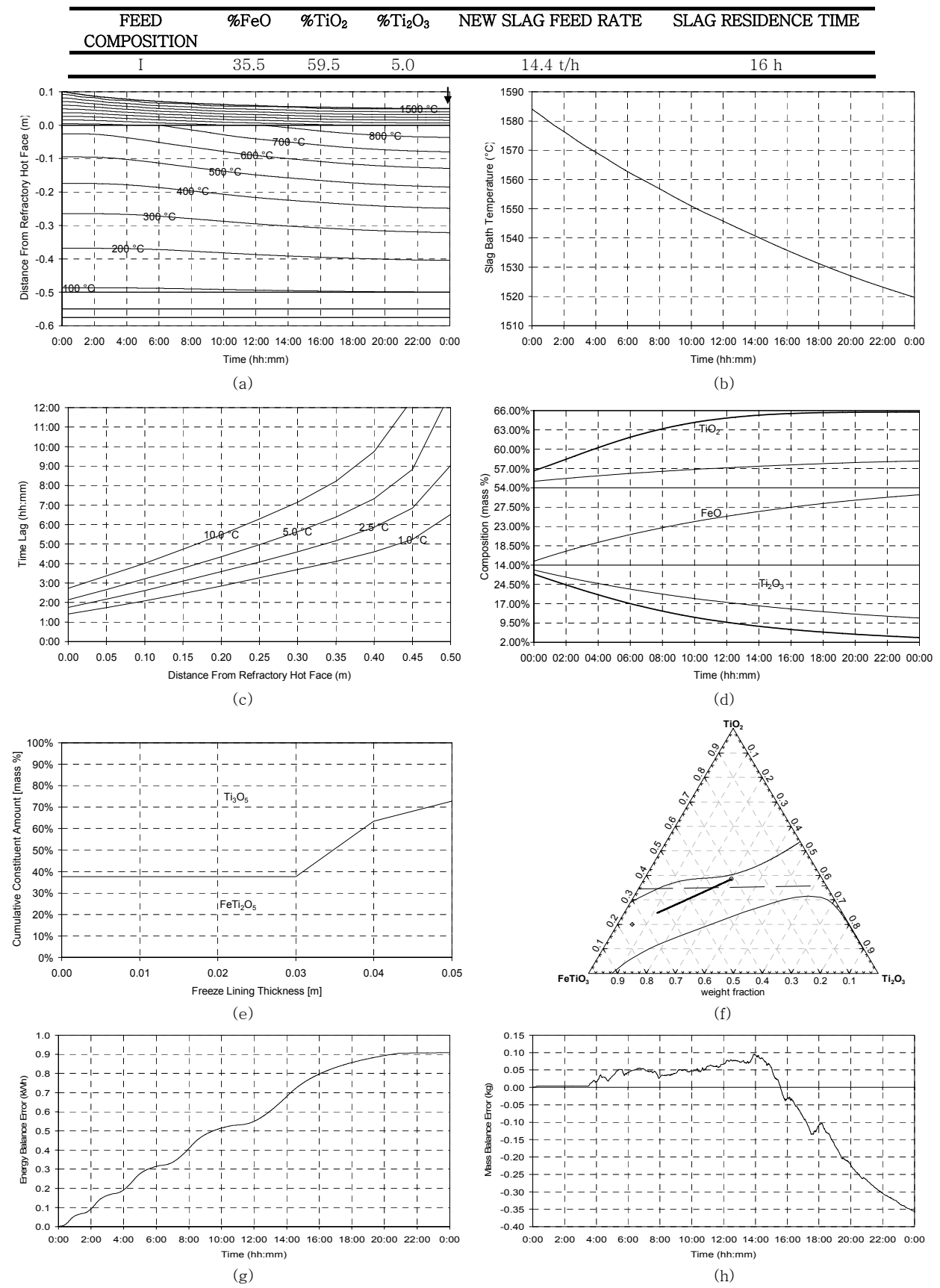


Figure 119 – Experiment 7.29 results.

## 7.3.30 Experiment 7.30

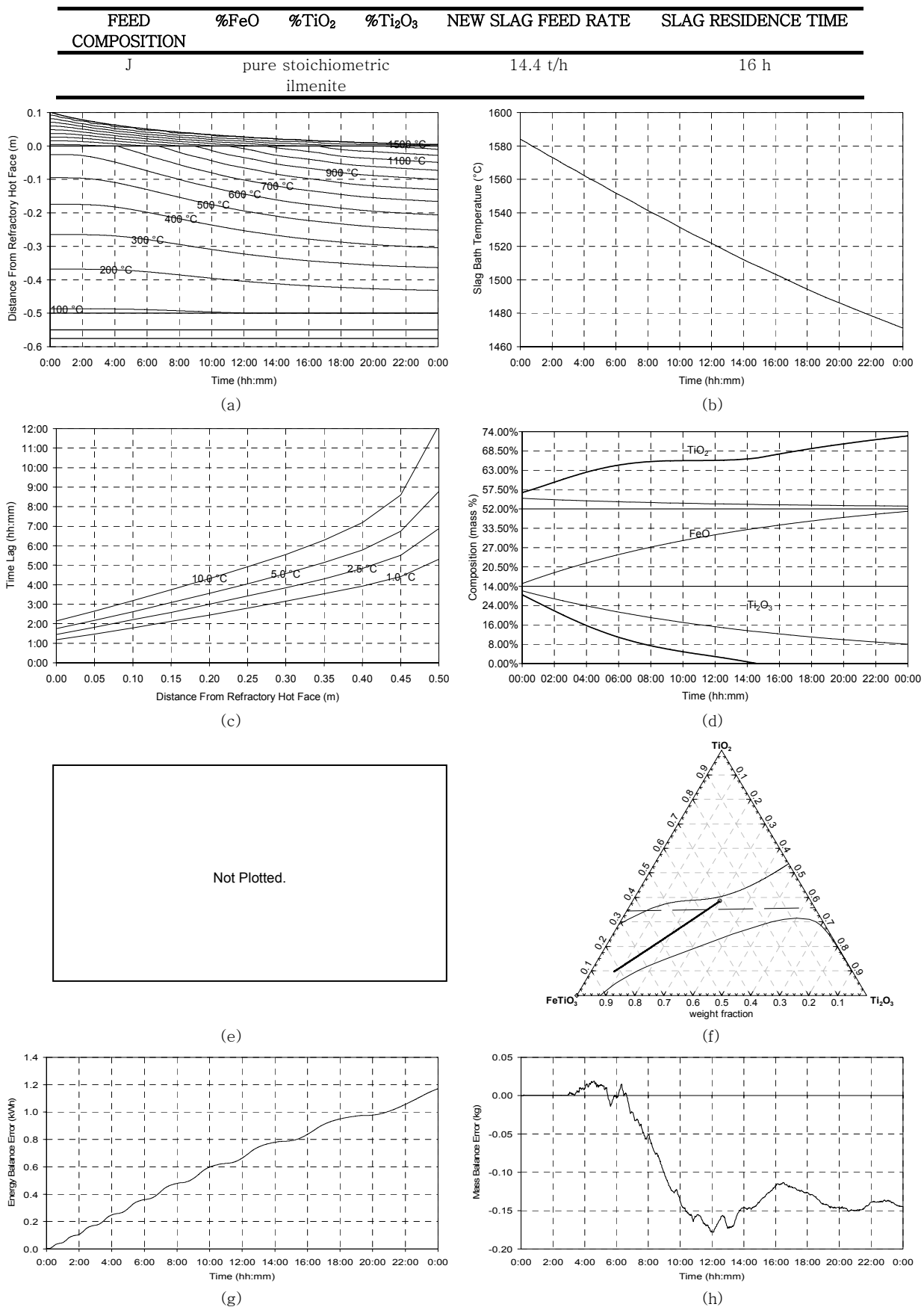


Figure 120 – Experiment 7.30 results.

## 7.4 DISCUSSION

One of the objectives of the set of experiments was to isolate the influence of slag composition on the interaction between slag bath and freeze lining as much as possible so that it can be studied clearly. Because heat transfer plays such a significant role in the system being considered in this chapter, its influence could not be completely removed from the experiments conducted. This is clear from the experimental results, especially in those of experiments 7.1 to 7.10 where the slag feed rate was set extremely high.

Before discussing the results in detail, the expected behaviour of the system must be considered. New liquid slag with composition different from the initial composition of the slag bath is fed into the system. The slag is ideally mixed in the SlagBath mixer and then extracted by the SlagTap material output module. The expected behaviour of such a system is that the composition of the slag bath will ultimately become equal to the composition of the new slag being fed. As a result of the changing slag composition, the liquidus temperature of the slag should change according to the liquidus surface of the system (as shown in Figure 11 on page 23) while its composition is moving from the initial to the new slag composition. The changing state of the slag bath should therefore influence the interface between the freeze lining and slag bath in two ways.

Firstly there is a thermal influence. It is expected, purely from heat transfer considerations, that the freeze lining will grow thicker when the slag bath temperature increases, and thinner when the slag bath temperature decreases. This statement takes into account that the slag bath temperature is always very nearly equal to the slag's liquidus temperature, that slag is fed at the current bath temperature, and that the power input into the system was kept constant at 250 kW. Hotter slag thus implies a lower rate of heat loss.

The second influence is a chemical one. The changing composition of the slag bath changes the compositional combination of solid slag and liquid slag that are present at the interface between the freeze lining and slag bath. If the composition of the new slag being fed is decreasing the liquidus temperature of the slag, the liquidus temperature of the combination of material at the interface is also likely to drop. This will result in solid slag being dissolved in the slag bath and in a thinner freeze lining. The opposite is expected if the liquidus temperature of the slag bath is increased by the new slag being fed.

It is therefore expected – based on both thermal and compositional considerations – that an increase in slag bath temperature will be associated with an increase in freeze lining thickness, and a decrease in slag bath temperature will be associated with thinner freeze lining to become thinner.

### 7.4.1 Freeze Lining Thickness

In most of the experiments, the above-mentioned expected influence of the new slag on freeze lining thickness was observed. The best examples are the results of experiments 7.2, 7.12 and 7.22. In these experiments the slag bath liquidus temperature first dropped as the composition approached the eutectic groove, and then started to rise after the eutectic groove had been crossed. As expected, the freeze lining thickness first decreased slightly and then became thicker.

The results of experiments 7.4 and 7.8 (and, to a lesser extent, experiments 7.6, 7.9, 7.14 and 7.16) appeared to display behaviour contrary to what was expected. Generally in these cases, a slight decrease followed by an increase in freeze lining thickness was observed even though the slag bath temperature decreased by 15 to 20 °C. It is not clear what the reason for this is, but it is likely related to the sharp increase in FeO content of the slag in all of these cases, which causes the slag liquidus temperature to drop. There is also an effect of the time lag in heat transfer changes, as discussed below.

Also of interest are cases (7.3, 7.5 and 7.7) where the freeze lining, in line with expectations, became thicker, but after some time started to become thinner. The origin of opposite trends with time (7.4, 7.6, 7.8 and 7.9) is likely to be related. The cases mentioned are all from the first subset where the highest feed rate was used. The same tendencies were either less pronounced or not present at all in the results of corresponding experiments executed with lower slag feed rates.

The reason for the observed increase and subsequent decrease in freeze lining thickness as well as the opposite behaviour is the difference in the dynamics of the thermal and chemical influences identified above. Because of the slag bath being well-mixed, the chemical influence of liquid slag on the freeze lining causes the freeze lining to grow thicker or thinner virtually immediately when a compositional change takes place. The thermal influence, however, is subject to the inertia of heat transfer through the furnace wall and freeze lining.

Experiment 7.5 is used as an example. The new slag used in this experiment has a liquidus temperature that is about 45 °C higher than the initial slag. The temperature of the slag bath immediately started increasing once the new slag was introduced. As expected, the freeze lining thickness also started to increase. The increase in thickness continued for 10 hours and then started decreasing. Heat transfer stepped in and resulted in the decrease in freeze lining thickness. The reason is that the freeze lining thickness that had been established after 10 hours could not conduct heat out of the system at the rate of 250 kW that was used as an energy input into the system. The freeze lining started to become thinner to again establish a heat transfer steady state in which the 250 kW input is conducted out of the system through the freeze lining and furnace wall.

Experiment 7.9 is another clear example. In this case, however, the freeze lining first became thinner due to the chemical influence of the slag bath, and then grew thicker to establish a heat transfer configuration that could remove 250 kW from the system.

#### 7.4.2 Thermal Response of Freeze Lining and Furnace Wall

Because the freeze lining thickness changed very little in many of the experiments, and because it often both increased and decrease, the same type of analysis that was done in paragraph 6.4.2 on the experimental results of CHAPTER 6 was not possible here. The reader is referred to paragraph 6.4.2 for a discussion on the thermal response of the freeze lining and furnace wall.

#### 7.4.3 Slag Bath Composition

The slag bath consistently displayed the expected behaviour in terms the change in its composition. In all cases the composition changed with virtually a straight line trajectory on the ternary graph (f) of the

experimental results. The slag bath reached the composition of the new slag in cases with high feed rates, and it was still approaching the new slag composition after 24 hours in cases where low feed rates were used.

In cases where the slag composition crossed the eutectic groove, the trajectory followed the eutectic groove for a period of time. When the average direction of the trajectory was roughly perpendicular to the eutectic groove, the slag composition followed the eutectic groove for only a short period of time. When the average direction was more parallel to the eutectic groove, the slag composition followed the groove for longer periods of time.

#### 7.4.4 Slag Bath Temperature

The expected slag bath temperature changes were evident in the results of all the experiments. This temperature is simply a function of the slag bath composition, and it followed the liquidus temperature surface shown in Figure 11 on page 23.

#### 7.4.5 Freeze Lining Composition

The freeze lining consisted of pseudobrookite as the only phase for most of the cases (new slag compositions A, D, F, G, H, I, J) since these slag composition in these cases were below the eutectic groove. This resulted in pseudobrookite being the primary solidification phase. In a few of the cases (new slag compositions B, C and E) the slag bath composition crossed over the eutectic groove. Once this happened, rutile became the primary solidification phase. This behaviour can be clearly seen on graph (e) of the results of the various experiments.